TITLE:

Fatigue Strength of Metals under Alternating Stresses of Varying Amplitude

AUTHOR(S):

NISHIHARA, Toshio; YAMADA, Toshiro

Fatigue Strength of Metals under Alternating Stresses of Varying Amplitude

By

Toshio NISHIHARA and Toshiro YAMADA

Department of Mechanical Engineering

(Received April 30, 1956)

Abstract

The criterion on fatigue damage and the formulas which can predict the fatigue lives and fatigue limits of metallic members under alternating stresses of varying amplitude, are established. The fatigue tests under alternating stresses of varying amplitude were carried out by the specially designed testing machines of three types, using unnotched or notched specimens of low-carbon steel, high-carbon steel and duralumin. And it is concluded that the fatigue lives and fatigue limits of metals subjected to varying repeated stresses like this can be determined by the analysis introduced in this paper.

I Introduction

As is generally the case, many machine members are subjected to repeated stresses of varying amplitude under the mean stress level which is varying continuously, and some parts are subjected to occasional overstresses (the stresses over the fatigue limit under constant stress amplitude). It is important in both academic and practical sense to estimate the fatigue strength, i.e. the fatigue life and the fatigue limit of metallic members under the stress condition like this.

A number of workers[1][2][3][4][5][6][7] have investigated this problem, but none have established a rational formula which predicts the fatigue life and the fatigue limit of metal under varying repeated stresses. For the accurate determination of the fatigue strength in these cases, the new criterion and formula have been established by employing the idea of the fatigue damage and the stress history.

As was reported in the authors' previous papers[8][9], the fatigue tests under alternating stresses of varying amplitude had been carried out by specially designed testing machines with low-carbon steel, high-carbon steel and duralumin under three different amplitude patterns of stresses. These data were analyzed by means of the new theoretical formula and it was verified that the analytical fatigue life and fatigue limit under these varying repeated stresses agreed with the test results.

NOTATION

σ	Stress amplitude
σ_W	Fatigue limit under constant stress amplitude
σ_{Wv}	Fatigue limit under varying stress amplitude, which represents σ_{max}
σ'_w	Fatigue limit under rotary bending of constant stress amplitude
σ'_{wv}	Fatigue limit under rotary bending of varying stress amplitude
σ_0	Certain stress amplitude less than σ_W (σ which is less than or equal to σ_0 does produce neither fatigue damage nor work hardening)
σ_a	Mean value of varying stress amplitude
σ_r	$(\sigma_{max} - \sigma_{min})/2$
σ_{max}	Maximum value of σ in one loading cycle
σ_{min}	Minimum value of σ in one loading cycle
σ_{so}	Upper yield point, σ_{su} Lower yield point
A, D, A', B', R, R', a, b, m, and p_1	Constants
E	Elastic constant
F	Fatigue damage produced by one stress cycle
$F_{N'}$	Fatigue damage produced in the N'th stress cycle
$F_{eN'}$	Fatigue damage produced in the N'th stress cycle by the repetition of varying stresses less than σ_{su}
$F_{pN'}$	Fatigue damage produced in the N'th stress cycle by the repetition of varying stresses some of which are higher than σ_{su}
N'	Number of stress cycles
N	Number of stress cycles till fatigue fracture
N_t	Evaluated total sum of stress cycles till fatigue fracture
n	Cumulative frequency, i.e. total sum of stress cycles from the maximum stress σ_{max} to any stress σ in one loading cycle
$H(n)$	Function of n
$\psi(\sigma, N')$	Function of σ and N', which represents the change of F induced by the progressive work hardening; work hardening function
n_0	Value of n corresponding to σ_0
n_c	Total sum of stress cycles in one loading cycle
S	True stress
Z'	Number of loading cycles
Z	Number of loading cycles till fatigue fracture
α	Correction factor of fatigue life
φ	Ratio of length of yielded portion to unit length in extreme fiber of specimen at bending stress
ε	Elastic strain, ε_e Elastic strain at yield point in tension or compression
ε''	Strain at the end point of horizontal line in stress-strain diagram
ε'	Actual strain in extreme fiber of specimen
ε_p	Pure plastic strain
ε_{pu}	Pure plastic strain at lower yield point
$J_0(xi)$	Bessel function of xi

II Criterion on Fatigue Strength

2.1 The Function of Fatigue Damage and Stress History, the S-N Curve and the Fatigue Limit, for Constant Stress Amplitudes

The S-N curves of various sorts of steels for constant stress amplitude are represented by Eq. (1) over some range of stress amplitude.

$$\sigma = a \log_e N + b , \tag{1}$$

where σ is stress amplitude, N is the number of stress cycles till fracture, and a and b are constants.

From Eq. (1)

$$1/N = e^{\frac{-1}{a}\sigma + \frac{b}{a}} , \tag{2}$$

Let $-1/a = A$ and $b/a = D$, Eq. (2) becomes

$$1/N = e^{A\sigma + D} . \tag{3}$$

From Eq. (3) it will be assumed, as the first approximation, that the fatigue damage F which is produced by one cycle of stress σ is

$$F = e^{A\sigma + D} . \tag{4}$$

Further, F for notched specimens of steel and other non-ferrous metals may be represented by Eq. (5).

$$F = e^{A\sigma^{p_1} + D}$$
$$= \exp (A\sigma^{p_1} + D) , \tag{5}$$

where p_1 is another constant.

It is simple to study the characteristic of F for $p_1 = 1$ as the case of some metallic members. It can be assumed that the fatigue fracture for constant stress amplitude occurs when the summation of F becomes unity, as expressed by the equation

$$\Sigma F = 1 \quad \text{and then} \quad F \cdot N = 1 . \tag{6}$$

From Eq. (4) and Eq. (6)

$$\sigma = \frac{-1}{A} \log_e N - \frac{D}{A} . \tag{7}$$

Eq. (7) gives the S-N curve for some sorts of metals for the stress range beyond the fatigue limit.

However, the actual S-N curve is not straight but curved, and becomes horizontal at the stress level near fatigue limit σ_W. This may be because the function F changes with the value of stress and the number of stress cycles. Microscopic plastic strains are induced in metals by repeating stresses and the microscopic plastic regions become hard gradually by increasing number of stress cycles. Due to the work

hardening effect, the microscopic plastic strain produced in every stress cycle of its region becomes smaller for cycle after cycle, and the fatigue damage F of its region becomes small with increasing number of stress cycles.

These hypothesis had been explained by NISHIHARA and KOBAYASHI[10], but in the paper the work hardening was treated as a function of the number of stress cycles only. However, it may be supposed that the work hardening of microscopic plastic region develops with the increase of plastic strain or of stress amplitude in it, resulting in more fatigue damage F by greater stress amplitude. Therefore, the decreasing rate of F at the stage of increasing number of stress cycles becomes greater as the stress amplitude becomes great.

Thus, the change of the fatigue damage F is a function of both the stress amplitude and the number of stress cycles. Let N' denote the number of stress cycles and $\psi(\sigma, N')$ the function of σ and N', which represents the change of F due to the work hardening. Then the fatigue damage $F_{N'}$ which is produced in the N'th stress cycle is represented by Eq. (8)

$$F_{N'} = e^{A\sigma + D} \cdot \psi(\sigma, N') . \tag{8}$$

It has been reported[11][12][13][14][15] that the changes of crystal structure and mechanical properties were set up by the repeated stresses of the magnitude less than the fatigue limit. For example, NISHIHARA and KAWAMOTO have reported in their papers[11] that damaged zone could be seen in the specimens subjected to the repeated stresses 23 per cent below the fatigue limit of the material, not only in rotating bending tests but in reversed torsion tests.. It was also reported that the size of damaged zone was greater by the repetition of greater stresses and *vice versa*. Fig. 1 presents some examples of these results, where r is a radius of specimen and a is the breadth of the damaged zone.

From these experimental data it is understood that the microscopic plastic slips appear in metal crystals by repeating the stresses less than the fatigue limit. It results in the work hardening of that regions with increasing number of stress cycles. Because of the limitation for plastic

Fig. 1. Fatigued zone-repeated stress diagram.

deformation of the work hardened region, the slip develops step by step into the elastic regions in the vicinity even before the stress–strain curve of specimen loses lineality and the hysteresis curve begins to appear. Fig. 1 shows that the damaged region
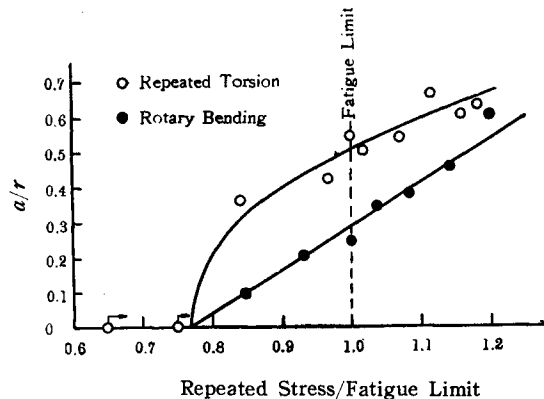
does not appear by repeating the stresses less than the 77 per cent of the fatigue limit.

Let σ_0 denote a certain stress amplitude less than the fatigue limit and assume that the repeated stress less than or equal to σ_0 does produce neither fatigue damage nor work hardening. Then, Eq. (8) becomes

$$\left.\begin{array}{ll}F_{N'}=e^{A\sigma+D}\cdot\psi(\sigma,\ N') & \text{at}\quad \sigma>\sigma_0 \\ F_{N'}=0, \qquad \psi(\sigma,\ N')=1 & \text{at}\quad \sigma\leqq\sigma_0 . \end{array}\right\} \qquad (9)$$

The calculation of $F_{N'}$ is not easy if the function $\psi(\sigma,\ N')$ is complex. As was mentioned before, the work hardening effect becomes greater with increasing σ. Then, assume that the fatigue damage produced in the next stress cycle decreases at the rate of $\exp(-m\sigma)$ due to the work hardening of the one cycle of stress σ, where m is a very small positive value.

And let $F_{N'-1}$ and $F_{N'}$ denote the fatigue damage F produced in the $(N'-1)$th and N'th stress cycles, respectively, then from the above assumption these relationship is represented by the equation

$$F_{N'}=F_{N'-1}\cdot e^{-m\sigma} . \qquad (10)$$

And then

$$F_1=e^{A\sigma+D} , \quad F_2=e^{A\sigma+D}\cdot e^{-m\sigma} , \quad F_3=e^{A\sigma+D}\cdot e^{-m\sigma\times 2} , \quad \cdots\cdots ,$$
$$F_{N'}=e^{A\sigma+D}\cdot e^{-m\sigma(N'-1)} .$$

Hence, $\psi(\sigma,\ N')$ has to be the form

$$\psi(\sigma,\ N')=e^{-m\sigma(N'-1)} . \qquad (11)$$

From Eq. (11), Eq. (9) becomes

$$\left.\begin{array}{ll}F_{N'}=e^{A\sigma+D}\cdot e^{-m\sigma(N'-1)} & \text{at}\quad \sigma>\sigma_0 , \\ F_{N'}=0 , \quad \psi(\sigma,\ N')=1 , & \text{at}\quad \sigma\leqq\sigma_0 , \end{array}\right\} \qquad (12)$$

where σ_0 is a certain value of stress smaller than the fatigue limit.

The condition for the fatigue fracture is assumed as

$$\int_0^N F_{N'}\cdot dN'=1 , \qquad (13)$$

where N is the number of stress cycles till fracture.

From Eq. (12) and Eq. (13), we have

$$e^{A\sigma+D}\int_0^N e^{-m\sigma(N'-1)}\cdot dN'=1 , \qquad \text{at}\ \ \sigma>\sigma_0 .$$

The solution is

$$\frac{e^{(A+m)\sigma+D}}{-m\sigma}\{e^{-m\sigma N}-1\}=1 .$$

Now, assume $m\ll A$ as is usually the case, then it becomes

$$\frac{e^{A\sigma+D}}{-m\sigma}\{e^{-m\sigma N}-1\}=1 , \qquad (14a)$$

or

$$N = \frac{-1}{m\sigma} \log_e \left\{ 1 - \frac{m\sigma}{e^{A\sigma+D}} \right\} . \tag{14b}$$

Eq. (14a) or Eq. (14b) represents the S–N relation for metals under constant stress amplitude. When σ is equal to the fatigue limit σ_W, N becomes infinite. In Eq. (14a), provided $N \to \infty$, i.e. $e^{-m\sigma_W N} = 0$, it follows

$$e^{A\sigma_W+D}/m\sigma_W = 1 .$$

Hence,

$$\log_e m = A\sigma_W + D - \log_e \sigma_W . \tag{15}$$

Eq. (15) is the condition for the repetition of the stress equal to the fatigue limit, and m can be determined by experiment as explained later.

When N is small, $m\sigma N$ is very small because m is the order of 10^{-8} as will be explained in the chapter which follows. For this case, it will be seen

$$e^{-m\sigma N} \doteqdot 1 - m\sigma N .$$

Then Eq. (14a) takes the form

$$\sigma = \frac{-1}{A} \log_e N - \frac{D}{A} . \tag{16}$$

Eq. (16) is the same as Eq. (7) and shows that σ *versus* $\log_e N$ relation is linear when N is small. The constants A and D can be determined from the straight line of the S–N curve in the range of small N. When A and D are thus determined, m can be obtained from Eq. (15), using the value of σ_W determined by experiment.

2.2 The Fatigue Life under Alternating Stresses of Varying Amplitude

The function $F_{N'}$ of the fatigue damage expressed in Eq. (12) can be applied not only for the case of constant stress amplitude but also for varying stress amplitude.

Let n denote the total sum of cycles of various stresses between the maximum stress $\sigma_{\max}$ and any stress σ in one loading cycle, i.e. the cumulative frequency for σ as illustrated in Figs. 10, 13 and 16. Then the relation of σ to n can be represented by the function

$$\sigma = H(n) . \tag{17}$$

The $\sigma - n$ diagram is called the stress−cumulative frequency diagram or simply the stress−frequency diagram (e.g. Fig. 10). Let n_c denote the total sum of stress cycles in one loading cycle, and n_0 the value of n corresponding to the stress σ_0 in the $\sigma - n$ diagram. Denoting Z' as the number of repeated loading cycles, the relation of N', Z', n_c and n takes the form

$$N' = n_c(Z'-1) + n . \tag{18}$$

As mentioned in Section 2. 1, the rate of work hardening in one cycle of stress σ can be assumed as $\exp(-m\sigma)$. Therefore, the work hardening function $\psi(\sigma, N')$ for alternating stresses of varying amplitude becomes, from Eq. (10), Eq. (12) and Eq. (18)

$$\psi(\sigma, N') = \exp\left[(Z'-1)\int_0^{n_0} -m\sigma \cdot dn + \int_0^{n-1} -m\sigma \cdot dn\right]. \tag{19}$$

It can be assumed that Z' is very great in general. Then, in Eq. (19)

$$\left|(Z'-1)\int_0^{n_0} -m\sigma \cdot dn\right| \gg \left|\int_0^{n-1} -m\sigma \cdot dn\right|.$$

Hence, from Eq. (19) it follows

$$\psi(\sigma, N') = \exp\left[-m(Z'-1)\int_0^{n_0}\sigma \cdot dn\right]. \tag{20}$$

Substituting Eq. (17) into Eq. (20), we obtain

$$\psi(\sigma, N') = \exp\left[-m(Z'-1)\int_0^{n_0}H(n)dn\right]. \tag{21}$$

$F_{N'}$, the fatigue damage which is produced in the N'th stress cycle, takes the form

$$F_{N'} = \exp(A\sigma + D) \cdot \exp\left[-m(Z'-1)\int_0^{n_0}H(n)dn\right]. \tag{22}$$

Putting

$$\int_0^{n_0}H(n)dn = Q, \tag{23}$$

Eq. (22) becomes

$$F_{N'} = \exp(A\sigma + D) \cdot \exp[-mQ(Z'-1)]. \tag{24}$$

Let $F_{Z'}$ denote the total sum of $F_{N'}$ which is produced in the Z'th loading cycle, it follows

$$F_{Z'} = \int_0^{n_0}F_{N'} \cdot dn.$$

From the above equation and Eq. (24) it will be seen that

$$F_{Z'} = \exp[-mQ(Z'-1)] \cdot \int_0^{n_0}\exp(A\sigma + D)dn$$

$$= \exp[-mQ(Z'-1)] \cdot \int_0^{n_0}\exp[AH(n) + D]dn. \tag{25}$$

Putting

$$\int_0^{n_0}\exp[AH(n) + D]dn = I, \tag{26}$$

Eq. (25) becomes

$$F_{Z'} = \exp[-mQ(Z'-1)] \cdot I. \tag{27}$$

Let Z be the total number of loading cycles till fatigue fracture, then the condition of fatigue fracture can be given by

$$\int_0^Z F_{Z'} \cdot dZ' = 1. \tag{28}$$

From Eq. (27) and Eq. (28), it follows that

$$I\int_0^Z \exp\left[-mQ(Z'-1)\right]dZ' = 1 \,.$$

Consequently

$$\frac{-I \cdot \exp(mQ)}{mQ}\{\exp(-mQZ)-1\} = 1 \,. \tag{29}$$

Moreover, as mQ is very small, $\exp(mQ) \fallingdotseq 1$. Hence, the above equation becomes

$$\frac{-I}{mQ}\{\exp(-mQZ)-1\} = 1 \,. \tag{30a}$$

Rearranging this

$$Z = \frac{-1}{mQ}\log_e\left\{1-\frac{mQ}{I}\right\} \,. \tag{30b}$$

Let N_t be the evaluated total sum of stress cycles till fatigue fracture, we have

$$N_t = n_c \cdot Z \,.$$

Substituting Eq. (30b) into the above equation, it is obtained

$$N_t = \frac{-n_c}{mQ}\log_e\left\{1-\frac{mQ}{I}\right\} \,. \tag{31}$$

Eq. (31) is the formula which gives the fatigue life N_t under alternating stresses of varying amplitude. To evaluate N_t by Eq. (31), Q and I must be known, resulting in necessitating the value of σ_0 which gives n_0. It is difficult to determine the value of σ_0 theoretically, because σ_0 is thought to vary according to the sort of material, heat treatment, form of specimen and so on. On the other hand σ_0 can be determined by experiment. For example, according to NISHIHARA and KAWAMOTO[11] who carried out the experiments to detect the damaged zone by a corrosion method, using Swedish 0.09 per cent carbon steel, the value of σ_0 was 76 per cent of the fatigue limit σ_W for constant stress amplitude of both rotating bending stress and reversed torsional stress. F. Wever and others[15] have obtained the same results that σ_0 is $0.76\,\sigma_W$. Therefore, it is here assumed that the value of σ_0 is $70\sim80$ per cent of the fatigue limit σ_W.

2.3 Simplified Formulas for Fatigue Lives

In the case of estimating the fatigue life, the values of N_t and Z at N_t are generally small, and so the value of mQZ is also small.

Then
$$\exp(-mQZ) \fallingdotseq 1-mQZ \,.$$

From Eq. (30a)
$$Z = 1/I \,,$$

and
$$\begin{aligned}
N_t &= n_c \cdot Z = n_c/I \\
&= n_c \Big/ \int_0^{n_0} \exp[AH(n)+D] \cdot dn
\end{aligned}$$

or
$$= n_c \Big/ \int_0^{n_0} \exp(A\sigma+D) \cdot dn \,. \tag{32}$$

Eq. (32) is the simplified formula to evaluate the fatigue life N_t.

Moreover, when σ is sufficiently great and N is small, $1/N$ is approximated as follows, from Eq. (16),

$$1/N = \exp(A\sigma + D) .$$

Applying the above relation through all the stress range, Eq. (32) takes the form

$$N_t = n_c \bigg/ \int_0^{n_0} \frac{dn}{N} ,$$

where $1/N = \exp(A\sigma + D)$ and $\sigma_0 = (0.7 \sim 0.8)\sigma_W .$ \hfill (33)

In oder to simplify the calculation, Eq. (33) can be more simplified as follows

$$N_t = n_c \bigg/ \int_0^{n_c} \frac{dn}{N} ,$$

where $1/N = \exp(A\sigma + D)$ and $1/N = 0$ at $\sigma \leq \sigma_W .$ \hfill (34)

On the other hand, employing the S-N curves obtained experimentally for constant stress amplitude, another formula for N_t is derived from Eq. (34) as

$$N_t = n_c \bigg/ \int_0^{n_c} \frac{dn}{N} ,$$

where $1/N = 0$ at $\sigma \leq \sigma_W$ and N is the value corresponding to σ on the S-N curve.   \hfill (35)

2.4 The Fatigue Limit under Alternating Stresses of Varying Amplitude

As is generally the case, many machine members are subjected to varying repeated stresses, and some of them are often subjected to overstresses. Some of test results[6] have reported that the fatigue limit of metal under alternating stresses of varying amplitude is higher than the original fatigue limit σ_W for constant stress amplitude. And some papers[16][17][18][19] show coaxing effect, that is, the increase of fatigue limit of the metal which had been prestressed by some understresses. These phenomena can be analyzed by means of the function of fatigue damage.

The fatigue limit under varying repeated stresses is denoted as σ_{Wv}, and can be evaluated as follows. The condition of fatigue limit under varying repeated stresses is that Z is infinite at Eq. (30a). When $Z \to \infty$, $\exp(-mQZ) = 0$.
Then Eq. (30a) has the form

$$I/mQ = 1 .$$ \hfill (36)

The fatigue limit under alternating stresses of varying amplitude can be given by Eq. (36), as A, D and m are known quantities from the experimental S-N curve for constant stress amplitude. The examples of calculation for this case will be related in Chapter III.

2.5 Example of Calculation

(The fatigue strength when the $\sigma - n$ curve is cosinusoid)

Fig. 8 in Chapter III shows schematically the mode of stress variation, which is realized with the testing machine I specially designed by authors (Figs. 6 and 7 in Chapter III). The stress-cumulative frequency curve, i.e. the $\sigma - n$ curve, is a cosine curve as shown in Fig. 10.

In this case the $\sigma - n$ curve is represented as

$$\sigma = \sigma_a + \sigma_r \cos \frac{\pi}{n_c} n, \tag{37}$$

where σ_a is the mean value of the varying stress amplitude and σ_r is the amplitude of the stress variation as explained in Fig. 8.

Substituting Eq.(37) into Eq.(23), we have

$$Q = n_0 \sigma_a + \frac{n_c}{\pi} \sigma_r \sin \frac{\pi n_0}{n_c}. \tag{38}$$

From Eq.(26) and Eq.(37), it follows

$$I = \exp\left[-\frac{1}{a}(\sigma_a - b)\right] \cdot \int_0^{n_0} \exp\left[-\frac{\sigma_r}{a}\cos\frac{\pi}{n_c}n\right] dn, \tag{39}$$

where $A = -1/a, \ D = b/a.$

Substituting Eqs.(38) and (39) into Eqs.(31) and (36) separately, the fatigue life and the fatigue limit in this case can be obtained. In the special case when the minimum stress amplitude, $\sigma_{\min}$, of varying stress is greater than σ_0, these formulas are simple as follows

$$\left.\begin{aligned} Q &= n_c \cdot \sigma_a \\ I &= n_c \cdot \exp\left[-\frac{1}{a}(\sigma_a - b)\right] \cdot J_0\left(\frac{\sigma_r}{a}i\right), \end{aligned}\right\} \tag{40}$$

and

$$N_t = \frac{-1}{m\sigma_a}\log_e\left\{1 - \frac{m\sigma_a}{\exp\left[-\frac{1}{a}(\sigma_a - b)\right] \cdot J_0\left(\frac{\sigma_r}{a}i\right)}\right\}. \tag{41}$$

The equation for the fatigue limit becomes

$$\frac{1}{m\sigma_a} \cdot \exp\left[-\frac{1}{a}(\sigma_a - b)\right] \cdot J_0\left(\frac{\sigma_r}{a}i\right) = 1. \tag{42}$$

Let σ_{aW} and σ_{rW} denote σ_a and σ_r respectively which satisfy Eq. (42), and the fatigue limit, σ_{Wv}, under varying stresses becomes

$$\sigma_{Wv} = \sigma_{aW} + \sigma_{rW}. \tag{43}$$

Further, according to the simplified formula Eq.(32), N_t becomes

$$\begin{aligned} N_t &= n_c/I \\ &= \exp\left[\frac{1}{a}(\sigma_a - b)\right]\bigg/ J_0\left(\frac{\sigma_r}{a}i\right). \end{aligned} \tag{44}$$

2.6   The Fatigue Life of Notched Specimens or Metal Members in which F is represented by $\exp{(A\sigma^{p_1} + D)}$

(1)   The S-N curve

In a notched specimen, plastic deformation occurs at the bottom of notch under a relatively low repeated nominal stresses, on account of the stress concentration. Therefore, the true stress at the bottom of notch is not only unproportional to the load, but also unproportional to the nominal stress which is computed by the formula of elasticity.   In these cases, the function of fatigue damage, F, should be represented by the form, employing Eq. (5),

$$F_{N'} = e^{A\sigma^{p_1} + D} \cdot e^{-m\sigma(N'-1)} . \qquad (45)$$

Now, in the discussion of fatigue life, N' is relatively small and it can be assumed as the first approximation that

$$\exp{[-m\sigma(N'-1)]} \doteqdot 1 .$$

Then Eq. (45) becomes

$$F_{N'} = \exp{(A\sigma^{p_1} + D)} . \qquad (46)$$

When fatigue fracture occurs at a number of stress cycles, N, it follows that

$$\Sigma F_{N'} = 1 \quad \text{and} \quad F_{N'} \cdot N = 1 .$$

Substituting Eq. (46) into the above equation, we find

$$\exp{(A\sigma^{p_1} + D)} \cdot N = 1 . \qquad (47a)$$

Rearranging this,

$$\sigma^{p_1} = \frac{-1}{A} \log_e N - \frac{D}{A} . \qquad (47b)$$

A, D and p_1 are constants which can be evaluated from the test data, and Eq. (47a) or (47b) represents the S-N curve for constant stress amplitude.   For example, p_1 can be evaluated from the values of two pair points on the experimental S-N curve.   The values of σ in each pair of test condition should have the same ratio r, for example, σ_k, $\sigma_k \cdot r$ and $\sigma_{k'}$, $\sigma_{k'} \cdot r$.

(2)   The Fatigue Life under Varying Repeated Stresses

If $F_{Z'}$ denote the total sum of $F_{N'}$ in the Z'th loading cycle,

$$F_{Z'} = \int_0^{n_c} F_{N'} \cdot dn .$$

Substituting Eq. (46) into the above equation, it is obtained

$$F_{Z'} = \int_0^{n_c} \exp{(A\sigma^{p_1} + D)} \cdot dn . \qquad (48)$$

From Eq. (47a) and Eq. (48), we have

$$F_{Z'} = \int_0^{n_c} \frac{dn}{N} , \quad \text{and} \quad F_{Z'} \cdot Z = 1 ,$$

from which it follows

$$N_t = n_c \cdot Z = n_c / F_{Z'} .$$

Finally
$$N_t = n_c \Big/ \int_0^{n_c} \frac{dn}{N} , \qquad (49)$$

where N is the number of stress cycles till fracture for constant stress amplitude. It is convenient to assume that

$$1/N = 0 \quad \text{at} \quad \sigma \leqq \sigma_W .$$

2.7 The Fatigue Life of Unnotched Specimen of Low-Carbon Steel Under Repeated Bending Stresses of Varying Amplitude, in the Case When the Maximum Stress is Between the Lower and Upper Yield Points

(1) The Mechanism of Local Yielding of Low-Carbon Steel Bar under Repeated Bending Stress

When a bar of low-carbon steel is subjected to static bending moment, the relation between the stress and strain is approximately linear untill the plastic deformation spreads all over the section.   And in the case of round bar, the yield point in bending is 1.6~1.7 times higher than the yield point in tension.   But in bending, when the stress at the extreme fiber of the bar exceeds the yield point in tension, the macro-scopic plastic deformation appears at the local parts of extreme fiber, resulting in the decrease of stress in that fiber to some value under the yield point, while the bar does not yield as the whole[20][21].   This phenomena of yielding can be interpreted by means of the assumption that is shown in Fig. 2.[20]   It can be assumed that the portion of φ in one unit length yields when the stress at the extreme fiber of specimen reaches the yield point as shown in Fig. 2.
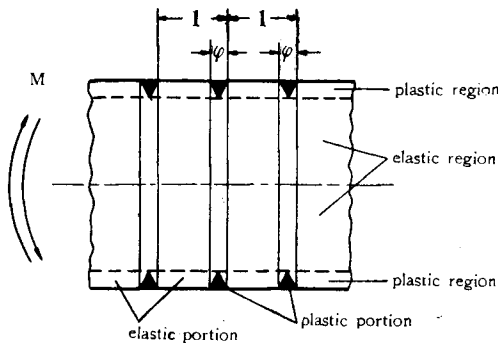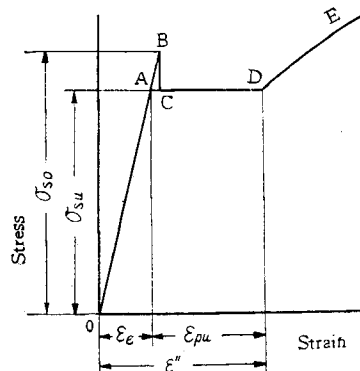

Fig. 2.

Fig. 3. Stress–strain diagram of low-carbon steel.

Denoting notations shown in Fig. 3, as

ε_e : elastic strain for the yield point in tension or compression (σ_{su}), $\varepsilon_e = \sigma_{su}/E$
   (E: elastic constant)

ε'' : strain at the end point of horizontal line in stress-strain diagram

ε' : actual strain in the extreme fiber of the specimen,

we have

$$\varepsilon' = (1-\varphi)\varepsilon_e + \varphi\varepsilon'' . \tag{50}$$

Let ε_{pu} denote the pure plastic strain at the lower yield point σ_{su}, and we have

$$\varepsilon'' = \varepsilon_e + \varepsilon_{pu} . \tag{51}$$

Then from Eq. (50) and Eq. (51), we obtain

$$\begin{aligned}\varepsilon' &= (1-\varphi)\varepsilon_e + \varphi(\varepsilon_e + \varepsilon_{pu}) \\ &= \varepsilon_e + \varphi\varepsilon_{pu} .\end{aligned} \tag{52}$$

Denote elastic strain in the elastic portion $(1-\varphi)$ as ε and pure plastic strain in the plastic portion φ as ε_p, for any true stress S. When the bending nominal stress σ reaches the value $+\sigma'$ which is between σ_{su} and σ_{s0}, the portion φ yields and its pure plastic strain becomes ε_{pu} as shown in Fig. 3.

When σ becomes $-\sigma'$ by reversed moment

$$\varepsilon' = \varphi \cdot \varepsilon_{pu} - \varphi \cdot \varepsilon_{pu} - \varepsilon_e = -\varepsilon_e . \tag{53}$$

The state expressed by Eq. (53) is shown at point G in Fig. 4. Points D and H in Fig. 4 show the state of stress and strain respectively in the case when the nominal stress σ of the specimen reaches $+\sigma'$ again or any stress lower than σ_{su}. These stress cycles shown in Fig. 4 will be repeated when the bending moment is reversed.

In this case of repeated bending stress of constant amplitude such as the rotating bending fatigue tests, let φ_0 denote the value of φ which is created by one cycle of σ', and take the case when $\sigma_{s0} > \sigma' \geqq \sigma_{su}$. Then from Eq. (52)

$$\varepsilon' = \varepsilon_e + \varphi_0\varepsilon_{pu} . \tag{54}$$

Because $\varepsilon_e = S/E$

$$\varepsilon' = S/E + \varphi_0\varepsilon_{pu} . \tag{55}$$

As the relation between the nominal stress σ' and the nominal strain ε' of the specimen is approximately linear, we have from Eq. (55)

$$\sigma'/E = S/E + \varphi_0\varepsilon_{pu} \quad \text{or} \quad S = \sigma' - E\varphi_0\varepsilon_{pu} . \tag{56}$$
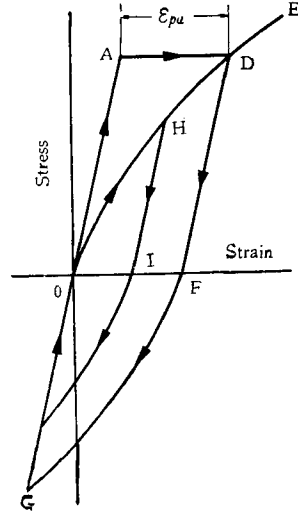

Fig. 4. Stress-strain diagram.

Eq. (56) shows that the true stress S is generally lower than the nominal stress σ' and S is lower than σ_{su} when σ' is equal to σ_{su}. This is the case of one stress cycle only. But when the number of these stress cycles increases, the plastic portions are subjected to work hardening by the repetition of plastic slip, resulting in the decrease of plastic strain.

Assuming that the plastic strain in the second stress cycle decreases at the rate of $\exp(-R\sigma')$, due to the work hardening which is produced during the first stress cycle of σ', the relation between the stress and the strain at the second stress cycle takes the form from Eq. (55)

$$\varepsilon' = S/E + \varphi_0 \varepsilon_{pu} \cdot e^{-R\sigma'} , \tag{57}$$

where R is the constant of small positive value.

And then, when the number of stress cycles becomes N', we may obtain

$$\varepsilon' = S/E + \varphi_0 \varepsilon_{pu} \cdot e^{-R\sigma'(N'-1)} . \tag{58}$$

The second term of the right hand side of Eq.(58) becomes smaller with the increase of stress cycle, N', and ε' is assumed to be constant during all stress cycles for repeated bending stress or rotating bending stress. Accordingly, the true stress S becomes higher with the increase of N'.

Assume that S becomes σ_{su} at $N'=N_1$ and then a part of the elastic portion in the extreme fiber of specimen yields more. Denoting φ_1 to be the value of the new plastic portion which is created in the N_1th stress cycle, we find

$$\varepsilon' = S/E + \varphi_0 \varepsilon_{pu} \cdot \exp[-R\sigma'(N_1-1)] + \varphi_1 \varepsilon_{pu} . \tag{59}$$

It can be assumed that the above mentioned phenomena occur step by step with the increase of N', i.e. $N'=N_1+N_2$, $N_1+N_2+N_3$, $\cdots$. Then we have at $N'=N_1+N_2+\cdots+N_i$,

$$\begin{aligned}
\varepsilon' = S/E &+ \varphi_0 \varepsilon_{pu} \cdot \exp[-R\sigma'(N_1+N_2+\cdots+N_i-1)] \\
&+ \varphi_1 \varepsilon_{pu} \cdot \exp[-R\sigma'(N_2+N_3+\cdots+N_i-1)] \\
&+ \cdots + \varphi_{i-1} \varepsilon_{pu} \cdot \exp[-R\sigma'(N_i-1)] \\
&+ \varphi_i \cdot \varepsilon_{pu} ,
\end{aligned} \tag{60}$$

where φ_1, φ_2, $\cdots$, φ_i are respectively the values of φ created when N_1, N_2, $\cdots$, N_i are added progressively.

Then
$$\Sigma\varphi = \varphi_0 + \varphi_1 + \varphi_2 + \cdots + \varphi_i . \tag{61}$$

$\Sigma\varphi$ becomes great with the increase of N' until $\Sigma\varphi$ reaches unity, but the specimen does not yield through its all section in this case.

(2) The Mechanism of Local Yielding of Low-Carbon Steel Bar under Repeated Bending Stress of Varying Amplitude ($\sigma_{\max} < \sigma_{s0}$)

Discussion is made on the general case, when the frequency of repeated stresses over the lower yield point, σ_{su}, is very small compared with that of the stresses less than σ_{su}.

After the plastic portion φ once appears by the few repetition of high stresses which exceed σ_{su}, the portion φ deforms plastically even by repeating stresses lower than σ_{su}. This phenomenon can be interpreted by taking account of that yielding of steel accompanies destruction of crystal bonds and it results in lowering the critical stress of subsequent yielding.

The relation between the stress σ and the pure plastic strain ε_p can be represented approximately by the equation[21]

$$\varepsilon_p = \exp (A'\sigma + B') , \tag{62}$$

where A' and B' are constants.

Let $\varphi_1, \varphi_2, \cdots, \varphi_i$ denote the values of φ produced respectively at the addition of loading cycles $Z_1, Z_2, \cdots, Z_i$, the relation between stress and strain in the $(Z_1 + Z_2 + \cdots + Z_i)$th loading cycle becomes in the same manner as before,

$$\begin{aligned}
\varepsilon' = S/E &+ \varphi_0 \exp (A'\sigma + B') \cdot \exp [-RQ(Z_1 + Z_2 + \cdots + Z_i - 1)] \\
&+ \varphi_1 \exp (A'\sigma + B') \cdot \exp [-RQ(Z_2 + Z_3 + \cdots + Z_i - 1)] + \cdots \cdots \\
&+ \varphi_{i-1} \exp (A'\sigma + B') \cdot \exp [-RQ(Z_i - 1)] \\
&+ \varphi_i \exp (A'\sigma + B') , \tag{63}
\end{aligned}$$

where

$$Q = \int_0^{n_c} \sigma \cdot dn = \int_0^{n_c} H(n) \, dn .$$

(3) The Fatigue Damage due to the Repetition of Macroscopic Plastic Deformation

It is understood that the fatigue damage is produced by the repetition of microscopic and macroscopic plastic deformation.

Let $F_{eN'}$ denote the fatigue damage produced in the N'th cycle of the stresses which are lower than σ_{su}, and $F_{pN'}$ the fatigue damage produced in the N'th cycle of stresses, some of which are higher than σ_{su} and create the local macroscopic plastic deformation. Then it is assumed that $F_{pN'} > F_{eN'}$. Therefore, we may have

$$\left. \begin{aligned} F_{pN'} &= \alpha F_{eN'} \\ \alpha &> 1 . \end{aligned} \right\} \tag{64}$$

It should be noted that when the maximum stress $\sigma_{\max}$ in varying repeated stresses is between σ_{su} and σ_{s0}, the initial macroscopic plastic portion φ which is not sufficiently work hardened is reserved during a large number of stress cycles, as shown by Eq. (63). But when a great number of repeated stresses which are higher than σ_{s0} are applied, as in the case of constant stress fatigue tests, for example, work hardening is great and $\Sigma\varphi$ becomes unity very early in the life of a specimen. The initial macroscopic plastic portion φ which has suffered to the fatigue damage $F_{pN'}$, thus changes itself into the microscopic plastic portion where the damage is $F_{eN'}$.

To simplify the computation, it is assumed that the plastic portion φ remains through all the life of a specimen when $\sigma_{s0} > \sigma_{\max} \geq \sigma_{su}$. Then from Eq. (12) and Eq. (64),

$$F_{eN'} = F_{N'} = e^{A\sigma + D} \cdot e^{-m\sigma(N'-1)}$$

$$F_{pN'} = \alpha \cdot F_{eN'} = \alpha \cdot e^{A\sigma + D} \cdot e^{-m\sigma(N'-1)} . \tag{65}$$

In the same manner as the derivation of Eq. (31), the formula of life is derived for this case, employing Eq. (65),

$$N_t = \frac{-n_c}{mQ} \log_e \left\{ 1 - \frac{mQ}{\alpha I} \right\} . \tag{66a}$$

The simplified formula, Eqs. (33), (34) and (35) in Section 2.3 becomes as follows:

$$N_t = n_c / \alpha \int_0^{n_0} \frac{dn}{N} ,$$
$$\text{where} \quad 1/N = \exp(A\sigma + D) , \quad \sigma_0 = (0.7 \sim 0.8)\sigma_W . \tag{66b}$$

$$N_t = n_c / \alpha \int_0^{n_c} \frac{dn}{N} ,$$
$$\text{where} \quad 1/N = \exp(A\sigma + D) , \quad 1/N = 0 \quad \text{at} \quad \sigma \leqq \sigma_W . \tag{66c}$$

$$N_t = n_c / \alpha \int_0^{n_c} \frac{dn}{N} ,$$
$$\text{where} \quad N = \text{fatigue life for } \sigma, \ 1/N = 0 \quad \text{at} \quad \sigma \leqq \sigma_W . \tag{66d}$$

The analysis of the experimental data in Chapter III, showed that $\alpha = 2$.

III Experimental Investigations

3.1 Materials and Specimens

The materials used were low-carbon steel, high-carbon steel and duralumin, having the chemical composition and the mechanical properties listed in Table 1 and Table 2, respectively. Both steels were tested in the "as received" condition and

Table 1. Chemical composition of metals tested, per cent

Material	C	Si	Mn	P	S	Fe	Ni	Cr	Cu	Mg	Al
Low-carbon steel	0.22	0.23	0.53	0.013	0.029	Remainder	—	—	—	—	—
High-carbon steel	0.61	0.25	0.61	0.044	0.026	Remainder	—	—	—	—	—
Duralumin	—	0.36	0.58	—	—	0.33	—	—	3.75	0.52	Remainder

Table 2. Mechanical properties of metals tested

Material	Upper yield point, kg/mm²	Lower yield point, kg/mm²	Tensile strength, kg/mm²	Breaking strength on final area, kg/mm²	Elongation, per cent	Reduction in area, per cent	Brinell hardness, (3000 kg. load)
Low-carbon steel	33.55	31.77	51.01	90.30	39	59.17	122.9
High-carbon steel	35.50	34.50	73.00	91.50	17.2	24.00	203
Duralumin	26.50*	—	41.10	—	25	—	—

* Yield strength, 0.2 per cent offset.

duralumin was water-quenched from
500°C 2 hours, and age hardened.
The fatigue studies included tests of
both notched and unnotched speci-
mens of the types shown in Fig. 5,
where (a) is for carbon steels, (b)
is for duralumin and (c), (d) are
for low-carbon steel.

3. 2　Fatigue Testing Machines

The three machines were used
to give the three different stress-
cumulative frequency curves. The
specially designed loading equip-
ments were attached to the rotary
bending testing machines to fluctuate
the stress amplitude.

(1)　The Fatigue Testing
Machine I

As shown in Fig. 6 and Fig. 7,

Fig. 5.　Dimensions of fatigue specimens.

the machines are composed of the rotary bending testing machine of nominal speed
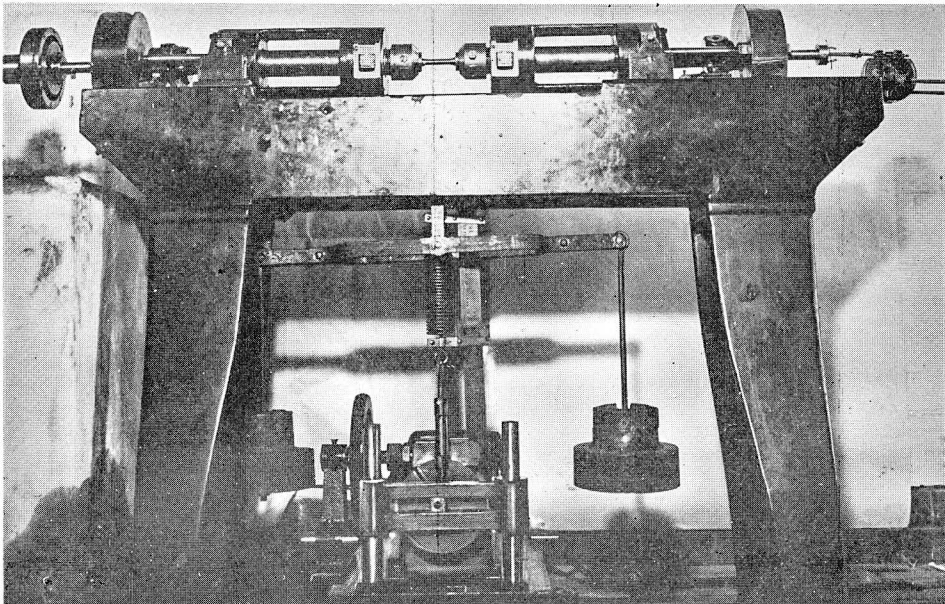
Fig. 6.　Rotary bending fatigue testing machine I, modified to apply Load Cycle I.

of 2000 rpm. and the specially designed loading equipment which gives cosinusoidally varying load to a specimen. The rotary bending testing machine gives alternating uniform bending stresses to a specimen, and the amplitude of which is fluctuated in cosine wave by the expansion and the contraction of the spring in the loading equipment. This equipment is composed of a spring and a rotating crank mechanism. A vertically sliding bar is moved periodically by the rotating crank arm which is rotated through a speed reducer, consisting of worm and worm wheel, and wheels driven by belt and motor.

Fig. 7. Set-up of rotary bending fatigue testing machine I, modified to apply Load Cycle I.

Then the motion of the sliding bar causes the periodical expansion and contraction of spring, so as to make a cosine wave of amplitude, and the spring force is directly applied to the loading unit of the testing machine. The mean amplitude of alternating stresses is given by the dead weights or the adequate initial expansion of the spring.
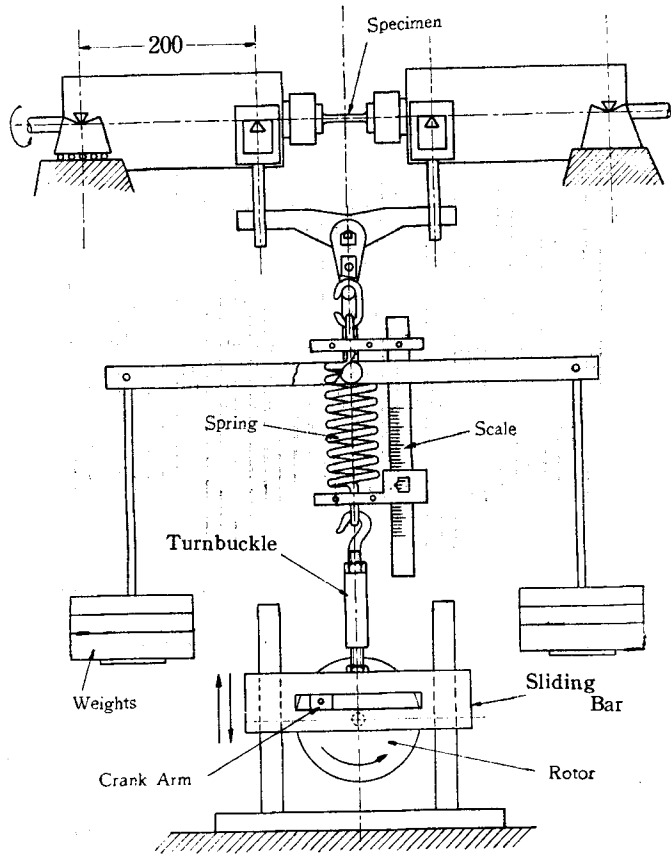
As the rotating speed of specimen (2000 rpm.) is very fast as compared with the rotating speed of the crank arm (9.3 rpm.), the amplitude of bending stresses in a specimen can be taken to vary as cosine wave. Fig. 8 shows the amplitude pattern of stresses developed by this machine, for one example of stress range. Dividing the amplitude of stresses in the steps of $0.5 \, kg/mm^2$, the stress–frequency diagram in Fig. 9 is obtained from Fig. 8. Further, the stress–cumulative frequency diagram can be obtained as shown in Fig. 10, which is a cosine curve (Load Cycle I).

The stress–cumulative frequency diagram, i.e. the relation between σ, σ_a, σ_r and n can be represented by the form
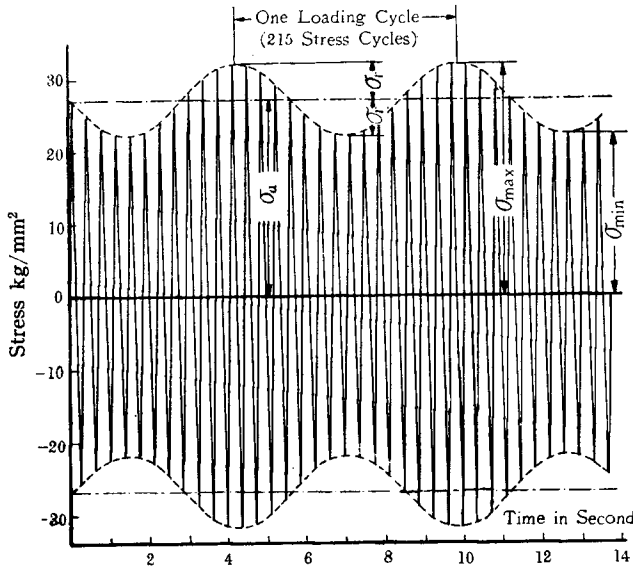
Fig. 8. Amplitude pattern of stresses developed by
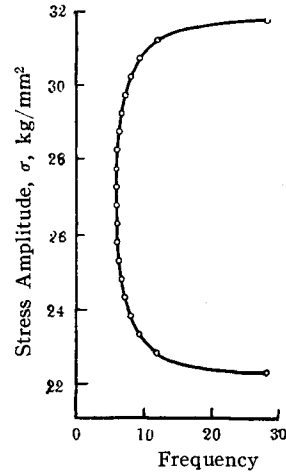machine I (Load Cycle I).
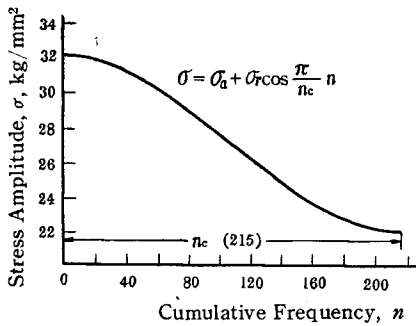

Fig. 9. Stress-frequency
diagram.

Fig. 10. Stress-cumulative frequency
diagram, Load Cycle I.

$$\sigma = \sigma_a + \sigma_r \cos \frac{\pi}{n_c} n , \qquad (37)$$

where n_c is taken to be about 215 in this case.

(2) The Fatigue Testing Machine II

As shown in Figs. 11 (a) and 11 (b) the manine II is also composed of the rotary bending testing machine and a loading equipment. In Fig. 11 (b) crank arm ① which rotates at the speed of 2.7 rpm. moves connecting rod ② and thus does a reciprocating motion of cam ③. The motion of cam ③ gives a vertical reciprocating motion of cam follower ④ which slides on two vertical guide bars and pressed to the cam by weights ⑤. The motion of the cam follower develops the periodical expansion and contraction of spring ⑥ which gives specimen ⑨ varying loads proportional to a strain of the spring. In conducting test, the desired minimum load is applied by weights ⑧ or the initial tension of spring ⑥ which is adjusted by turnbuckle ⑦. Adjustment of load range must be done by employing an adequate spring to secure certain stress-cumulative frequency curve through all tests. The rotating speed of specimen ⑨ is 1900 rpm. and a sum of stress cycles in one loading cycle (n_c) is about 703. Fig. 12 shows the amplitude pattern of stresses, developed by this machine. For this case, the stress-cumulative
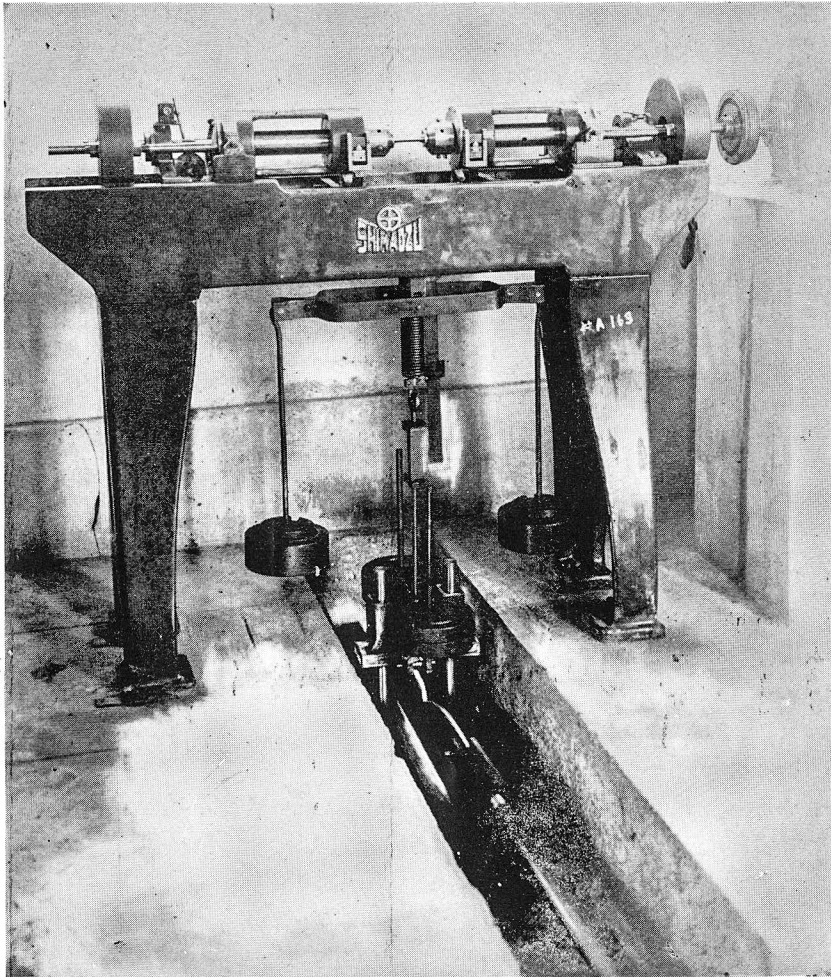
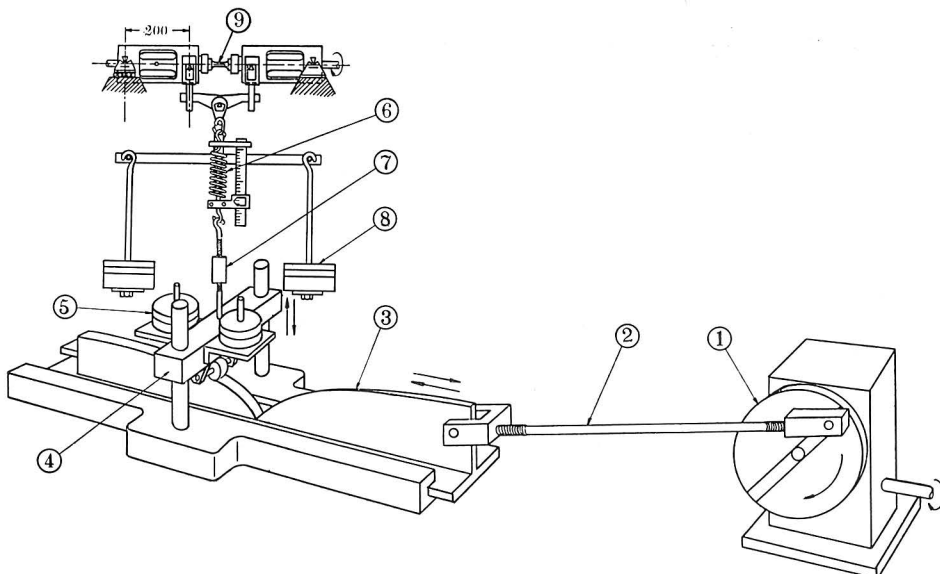Fig. 11 (a)   Rotary bending fatigue testing machine II, modified to apply Load Cycle II.

Fig. 11 (b)   Set-up of rotary bending fatigue testing machine II, modified to apply Load Cycle II.
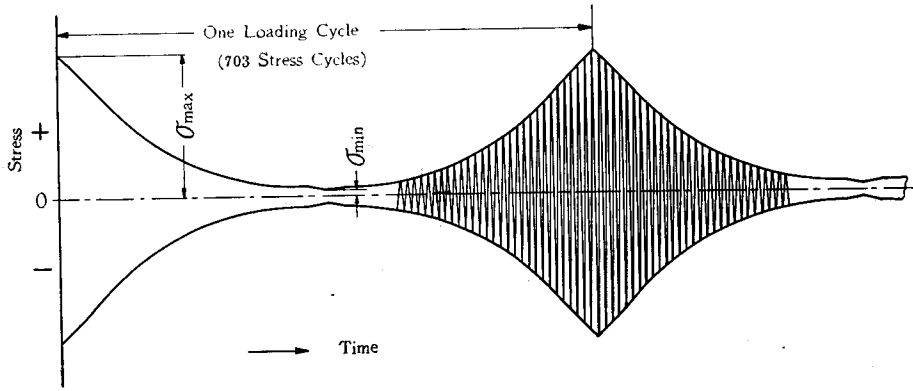
Fig. 12. Amplitude pattern of stresses, developed by machine II (Load Cycle II).

frequency diagram is shown in Fig. 13 (Load Cycle II).

(3) The Fatigue Testing Machine III

The another testing machine was made to develop the stress–cumulative frequency curve which is very similar to that of some aeroplanes. The general set-up of the machine is shown in Fig. 14. This machine is of the same type as the

Fig. 13. Stress–cumulative frequency diagram, Load Cycle II.

fatigue testing machine II illustrated in Figs. 11 (a) and 11 (b). Two levers ①, ② are added to magnify the load applied by the spring, and the weights shown in Fig. 11 (b)
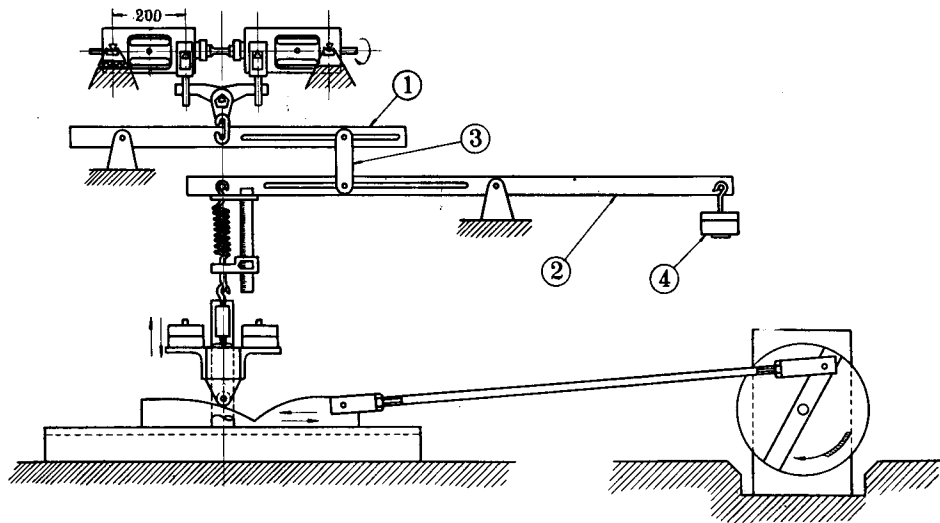
Fig. 14. Rotary bending fatigue testing machine III, modified to apply Load Cycle III.

were removed. In Fig. 14, ④ is counter weights which balance the weights of the spring and the levers, and therefore the minimum loads are made to be zero through all tests by using adequate weight for weight ④.

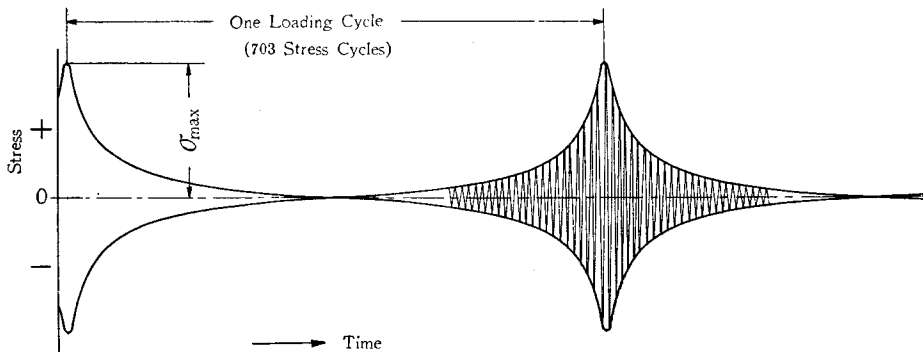In conducting test, the desired range of load can be applied by adjusting the

Fig. 15. Amplitude pattern of stresses, developed by machine III (Load Cycle III).

position of connecting bar ③ which connects levers ① and ②. The rotating speeds of specimen and crank arm are same as that of the fatigue testing machine II. The amplitude pattern of stresses developed by this machine is illustrated in Fig. 15, and the stress-cumulative frequency diagram for this case is shown in Fig. 16, (Load Cycle III), in which the measured values for some aeroplane are plotted for reference.

3.3 Test by the Fatigue Testing Machine I

(1) 0.22 Per Cent Carbon Steel (Unnotched Specimen)

Two groups of test specimens were produced from each of two round bars respectively, and were denoted by Group *A* and *B*. The shape of specimen is shown in Fig. 5 by (a).
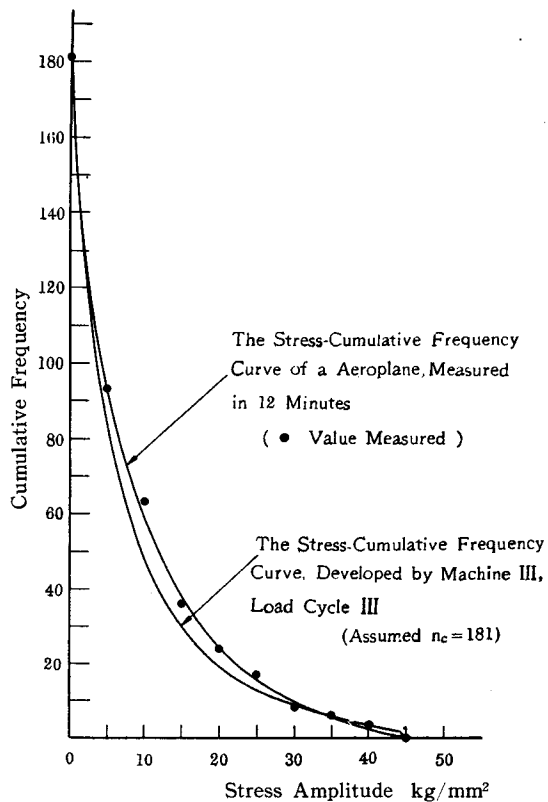

Fig. 16. Stress-cumulative frequency diagram, Load Cycle III.

a. Test with the specimens of Group A

The results of fatigue test under constant stress amplitudes are shown in Fig. 17 by solid circles, and the analytical S-N curve determined by using Eq. (14b) are shown by a solid line, by which the fatigue limit σ_w' was determined as 28.5 kg/mm^2.
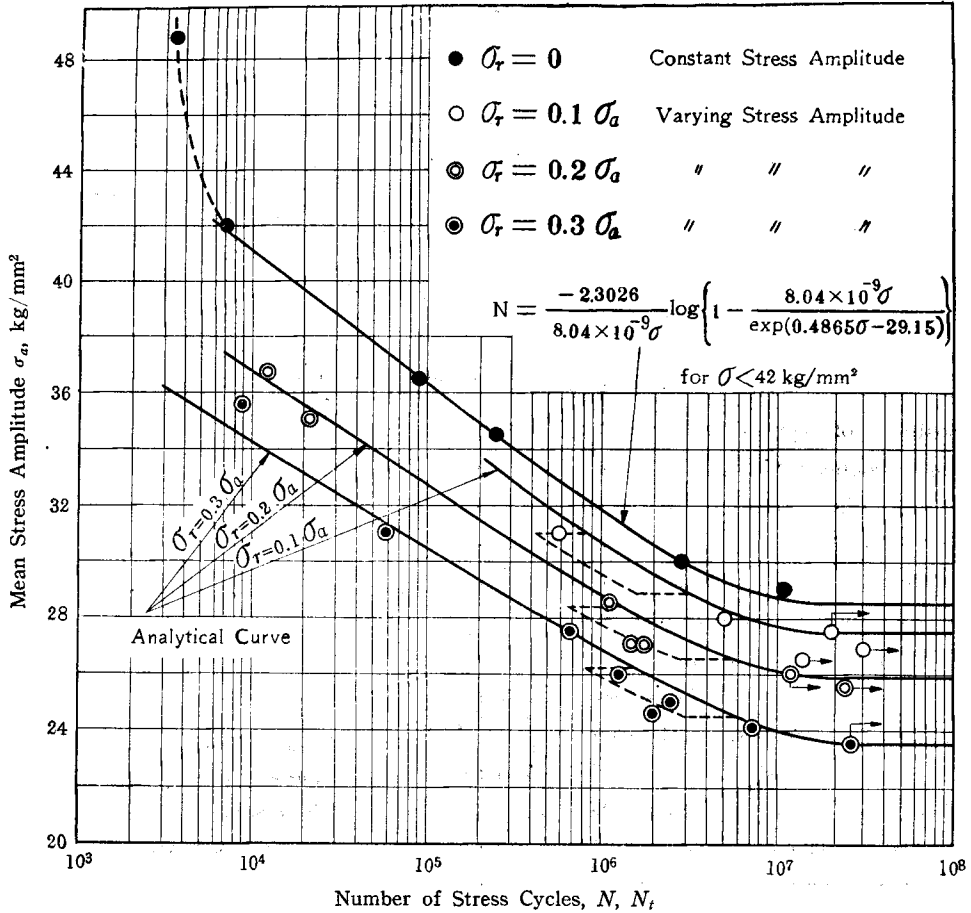

Fig. 17. Test results for unnotched specimens of 0.22% carbon steel
under Load Cycle I (Group A).

The computed values of coefficients A, D and m in Eq. (14b) are, $A = 0.4865$, $D = -29.15$ and $m = 8.04 \times 10^{-9}$. Then the analytical S-N relation for $\sigma < 42$ kg/mm^2 takes the form,

$$N = \frac{-2.3026}{8.04 \times 10^{-9}\sigma} \log \left\{ 1 - \frac{8.04 \times 10^{-9}\sigma}{(0.4865\sigma - 29.15)} \right\}.$$

The S-N curve determined by this equation agrees with the test results very well. The experimental S-N curve in the stress range for $\sigma \geq 42$ kg/mm^2 is shown by a dotted line in Fig. 17. It is seen that the S-N curve for this stress range is on the

right hand side of the extension of the analytical *S–N* curve on account of the phenomena that the specimens are subjected to repeated yielding when σ is greater than $42 \, kg/mm^2$, which is presumed to be the yield point in dynamic loading (repeated bending).

The fatigue tests for alternating stresses of varying amplitude were conducted for various values of σ_a combined with $\sigma_r = 0.1$, 0.2 and 0.3 σ_a, and the test results are shown by respective symbols in Fig. 17, where the ordinate represents the magnitude of the mean stress amplitude σ_a and the abscissa the sum of stress cycles till fracture.

The analytical fatigue life N_t and fatigue limit σ'_{wv} were computed by employing Eq. (31) and Eq. (36), and using the values of coefficients A, D and m thus determined, where the value of σ_0 was assumed as $\sigma_0 = 20 \, kg/mm^2 = 0.702 \, \sigma_w'$. The practical method of computation was described in Chapter II. The diagram representing the relation between the alternating stress of varying amplitude and the number of stress cycles till fracture, which is shown by plotting the mean stress amplitude σ_a against the number of cycles N_t with σ_r as parameter, might not be taken as ordinary *S–N* curve. For the convenience's sake, let us call the curve as "modified *S–N* curve". These analytical "modified *S–N* curves" are exhibited by three solid curves in Fig. 17. It should be noted that a fairly good agreement was obtained between the results of analysis and experiment not only for the fatigue lives but also for fatigue limits, with the exception of the stress range where the maximum value of the varying stress amplitudes was between the lower and the upper yield point of the steel.

The analytical fatigue limits in these cases are shown in Table 3. These fatigue limits, σ'_{wv}, are greater than the original fatigue limit, σ_w', for constant stress amplitude. It must be due to coaxing effect which is presented by lower stresses in varying stress amplitude, as explained before.

Table 3. Analytical fatigue limits of 0.22% carbon steel (Group A) under alternating stresses of varying amplitude (Load Cycle I).

Variation of stress amplitude	σ_{aW} kg/mm^2	σ_{rW} kg/mm^2	σ'_{wv} kg/mm^2
$\sigma_r = 0.1 \, \sigma_a$	27.53	2.75	30.28
$\sigma_r = 0.2 \, \sigma_a$	25.86	5.17	31.03
$\sigma_r = 0.3 \, \sigma_a$	23.52	7.06	30.58

(Original fatigue limit $\sigma_w' = 28.5 \, kg/mm^2$)

For the stress range where the maximum stress amplitude was between the lower and the upper yield point, the correction was made to evaluate the fatigue lives, employing Eq. (66a) in Section 2. 7, and applying the value of $\alpha = 2$. The fatigue lives thus computed are also shown in Fig. 17 by the fractions of dotted lines close to the respective solid curves. The deviation of the experimental results in this stress range from the solid lines is interpreted in this way.

The analysis described above is a little complex. It is simplified by employing

the simplified formula in Section 2.3 in place of Eq. (31). In this case, the fatigue lives, N_t, were determined by Eq. (33) and the thus determined "modified S-N curves" are shown by solid lines in Fig. 18. And alike in Fig. 17, for the stress range, $\sigma_{so} > \sigma_{max} \geqq \sigma_{su}$, the correction was made for these analytical fatigue lives, employing Eq. (66b) and the value $\alpha = 2$. The fatigue lives thus computed are shown in Fig. 18 by the dotted lines respectively. From the figure it is seen that the fatigue lives thus computed are equal to or a little smaller than the test results. Hence, the experimental fatigue lives are between the fatigue lives computed by Eqs. (31), (66a) and those by Eqs. (33), (66b). It may be mentioned that the fatigue lives determined from Eqs. (33), (66b) can be applied as the values of safety side in designing a machine member. The thin line which contacts with the analytical S-N curve, is the line due to the formula, $1/N = \exp(A\sigma + D)$.
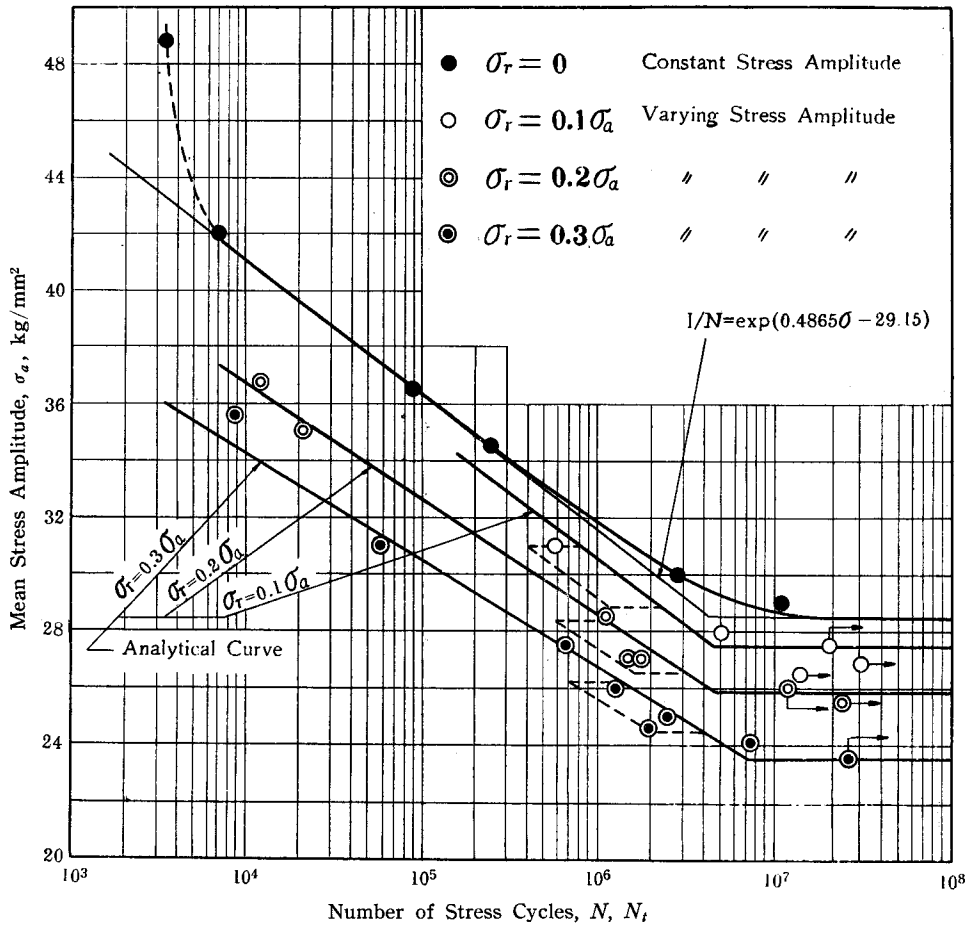

Fig. 18. Test results for unnotched specimens of 0.22% carbon steel under Load Cycle I (Group A).

b. Test with the specimens of Group B

The summary of the results of tests conducted are shown in Fig. 19 by various sorts of small circles. The fatigue limit σ_w' was determined to be 27.5 kg/mm². A straight line was drawn to represent a probable average of the test points for the tests of constant stress amplitude. From the oblique straight line thus drawn, the coefficients A, D and m were determined. $A = 0.4475$, $D = -27.02$ and $m = 1.466 \times 10^{-8}$.
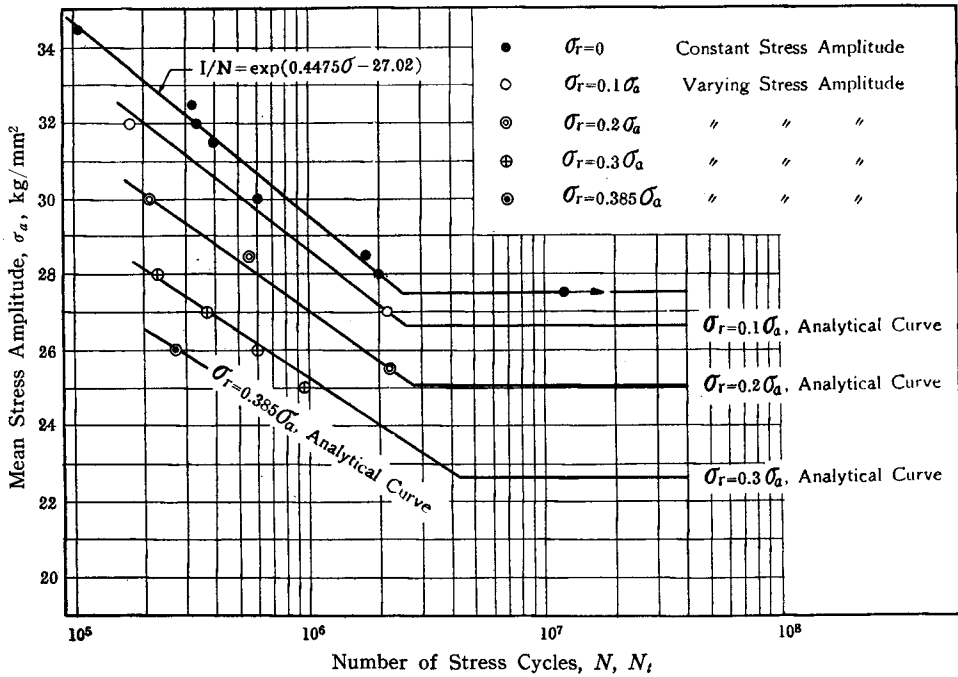

Fig. 19. Test results for unnotched specimens of 0.22% carbon steel under Load Cycle I (Group B).

The fatigue tests under alternating stresses of varying amplitude were conducted in the cases of $\sigma_r = 0.1$, 0.2, 0.3 and $0.385\,\sigma_a$. The analytical "modified S-N curves" for these cases were determined by employing the simplified formula Eq. (33) and demonstrated in Fig. 19 by solid lines. The analytical fatigue limits for these cases computed by Eq. (36) employing the value of $\sigma_0 = 20$ kg/mm² ($0.728\,\sigma_w'$), are also known from Fig. 19. It can be again noted that a fairly close agreement was obtained between the results of analysis and those of experiments in this case also.

(2) 0.61 Per Cent Carbon Steel (Unnotched Specimen)

Test specimens were made of two round bars of 0.61% carbon steel, the shape being shown in Fig. 5 by (a). The specimens were divided into two groups, A and B, according to the original bars.

a. Test with the specimens of Group A

The conventional fatigue test results and the analytical S–N curve are shown in Fig. 20 by solid circles and solid line respectively. The fatigue limit $\sigma_w{'}$ was determined as 27.8 kg/mm². And the analytical S–N curve for stress range of $\sigma<38$ kg/mm², was
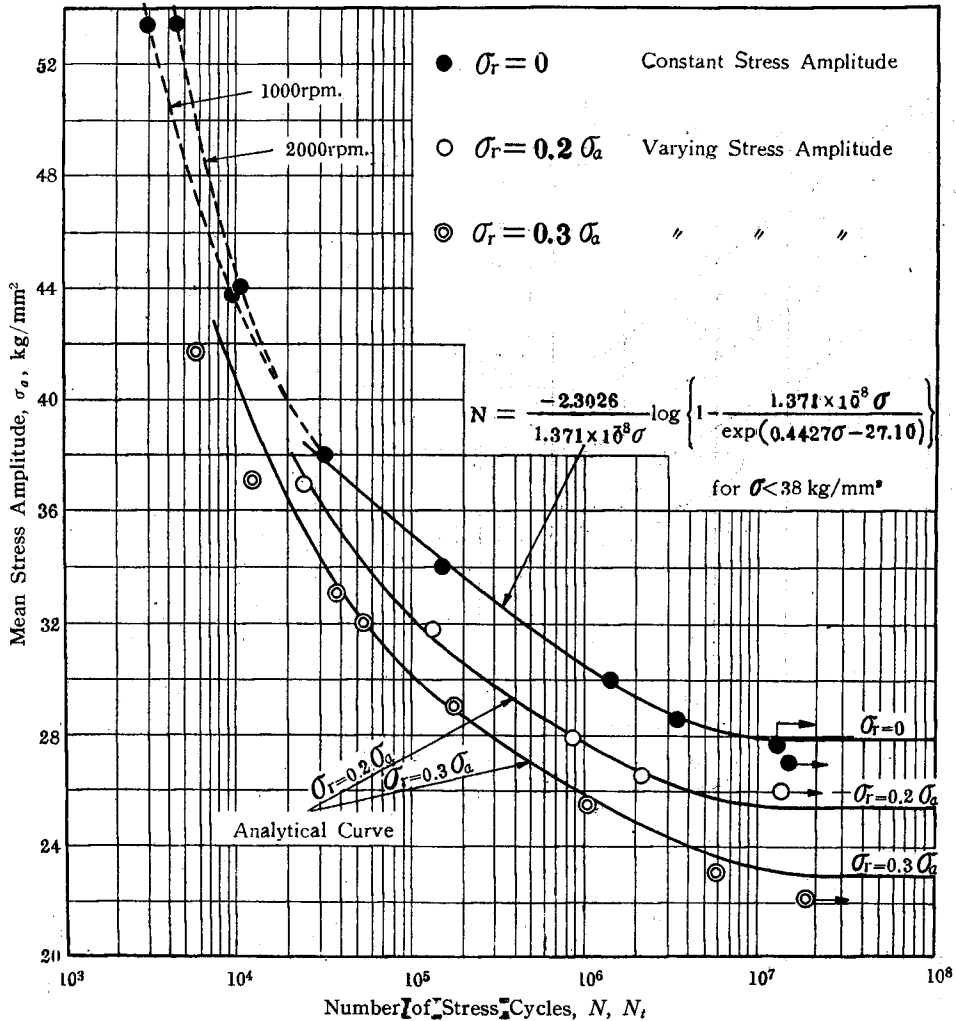

Fig. 20. Test results for unnotched specimens of 0.61% carbon steel under
Load Cycle I (Group A).

determined by means of Eq. (14b), by which the values of coefficients are determined as $A=0.4427$, $D=-27.10$ and $m=1.371\times10^{-8}$. The S–N relation for the stress range of $\sigma<38$ kg/mm², takes the form,

$$N=\frac{-2.3026}{1.371\times10^{-8}\,\sigma}\log\left\{1-\frac{1.371\times10^{-8}\,\sigma}{\exp\,(0.4427\sigma-27.10)}\right\}.$$

This formula shows a fairly close agreement with the test results, including the test points at the fatigue limit and its neighbourhood. Further, the fatigue tests of constant stress amplitudes at the two higher stresses of $\sigma = 53.46$, $43.85\,\text{kg/mm}^2$, were carried out, employing two different test speeds of 1000 rpm. and 2000 rpm. in order to study the effect of test speed on the fatigue lives. The test results are shown by the two curves of dotted lines in Fig. 20, which exhibit that the fatigue lives for the speed of 2000 rpm. were greater than that for the speed of 1000 rpm. During these tests, considerable amount of heat was produced in the specimens owing to the repetition of plastic deformation, and therefore it was seemed that the major effect of the test speeds was due to the heat produced, which caused the temperature rise in specimen. It is thus known that the increase of test speed causes heat in a specimen, resulting in longer fatigue life. From these tests, the value of dynamic yield point in bending of these specimens was estimated as $38\,\text{kg/mm}^2$. This is the reason why the experimental *S–N* curve deviates from the analytical *S–N* curve given by Eq. (14b) at the range of applied stress amplitude over $38\,\text{kg/mm}^2$.

The fatigue tests for alternating stresses of varying amplitude were conducted, under various values of σ_a with $\sigma_r = 0.2$ and $0.3\,\sigma_a$, and the results are shown in Fig. 20 by respective symbols. The analytical fatigue strengths were computed by means of Eqs. (31) and (36) in the stress range of $\sigma_{\max} < 38\,\text{kg/mm}^2$, and by Eq. (35) in the stress range of $\sigma_{\max} \geqq 38\,\text{kg/mm}^2$, where σ_0 was estimated as $20\,\text{kg/mm}^2$ ($= 0.72\,\sigma'_w$). These analytical values of fatigue strength are exhibited in Fig. 20 by the two solid curves, which are fairly close to experimental results. It should be noted that at the calculation by Eq. (35), the values of N were determined from the experimental *S–N* curve for the test speed of 1000 rpm., because quite a little amount of heat was produced in the fatigue test under the varying stress amplitude, owing to the fact that the frequency of high stress amplitude was relatively small.

The values of the analytical fatigue limit in these cases are as follows:

$\sigma'_{wv} = 30.42\,\text{kg/mm}^2$ when $\sigma_r = 0.2\,\sigma_a$, $\sigma'_{wv} = 29.85\,\text{kg/mm}^2$ when $\sigma_r = 0.3\,\sigma_a$.

It should be emphasized that these values of analytical fatigue limit σ'_{wv} are greater than the original fatigue limit σ'_w ($27.8\,\text{kg/mm}^2$) for constant stress amplitude, and σ'_{wv} have a good agreement with the test results as illustrated in Fig. 20.

Furthermore, the analytical fatigue lives under varying repeated stresses were computed by the simplified formula Eq. (33) in Section 2. 3, and the "modified *S–N* curves" are shown in Fig. 21 by solid lines. Alike in the case of 0.22% carbon steel, these fatigue lives given by use of Eq. (33) are on the safety side. The line of $1/N = \exp(A\sigma + D)$ is shown in the same figure by a thin line.

b. Test with the specimens of Group *B*

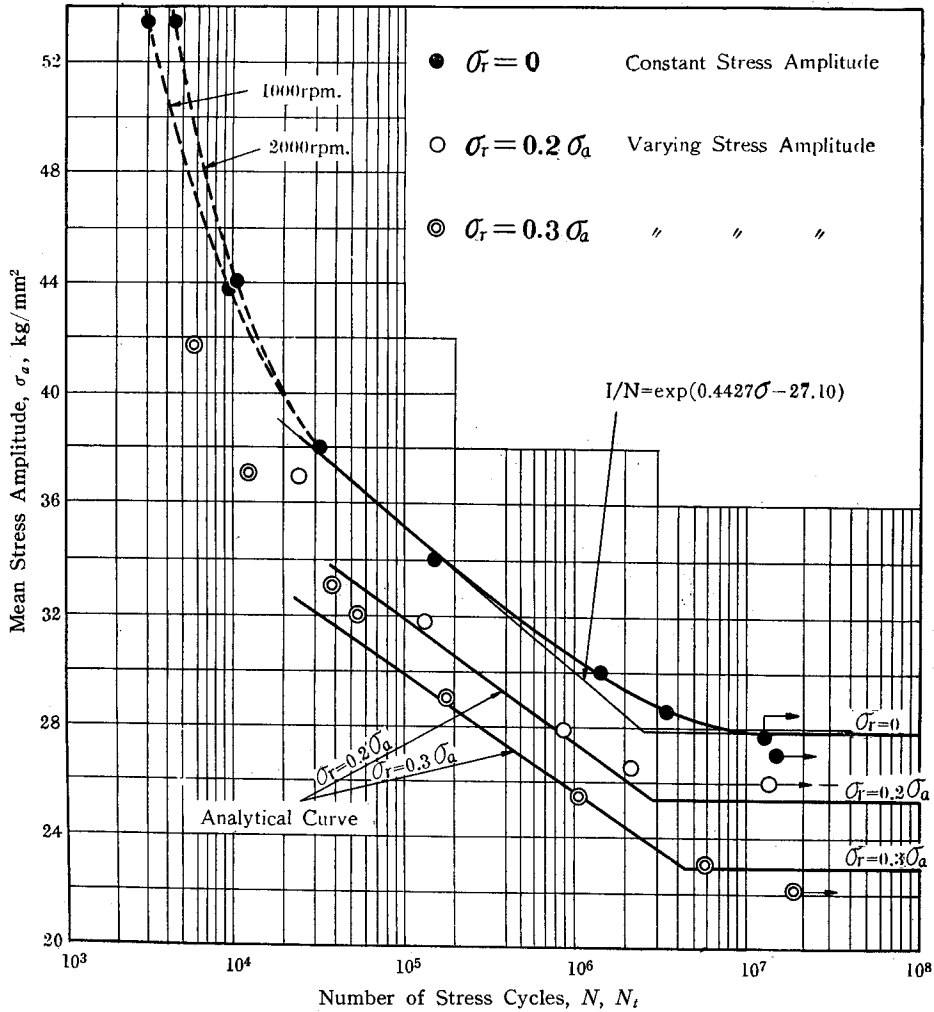The test results are plotted in the same manner as before and are shown in

Fig. 21.   Test results for unnotched specimens of 0.61% carbon steel under
Load Cycle I (Group A).

Fig. 22. The tests under constant stress amplitudes 55 and 47 kg/mm² were carried
out by the test speed of 1000 rpm. σ_w' was estimated as 29 kg/mm², and then $A=$
0.2558, $D=-20.43$, $m=7.73\times10^{-8}$ are obtained. Therefore, the analytical S–N relation
for the stress range of $\sigma < 46$ kg/mm² takes the form,

$$N=\frac{-2.3026}{7.73\times10^{-8}\sigma}\log\left\{1-\frac{7.73\times10^{-8}\sigma}{\exp\,(0.2558\,\sigma-20.43)}\right\},$$

and it has a fairly close agreement with the test results as shown in Fig. 22.

The analytical fatigue strength under varying repeated stresses for $\sigma_r=0.1\sigma_a$
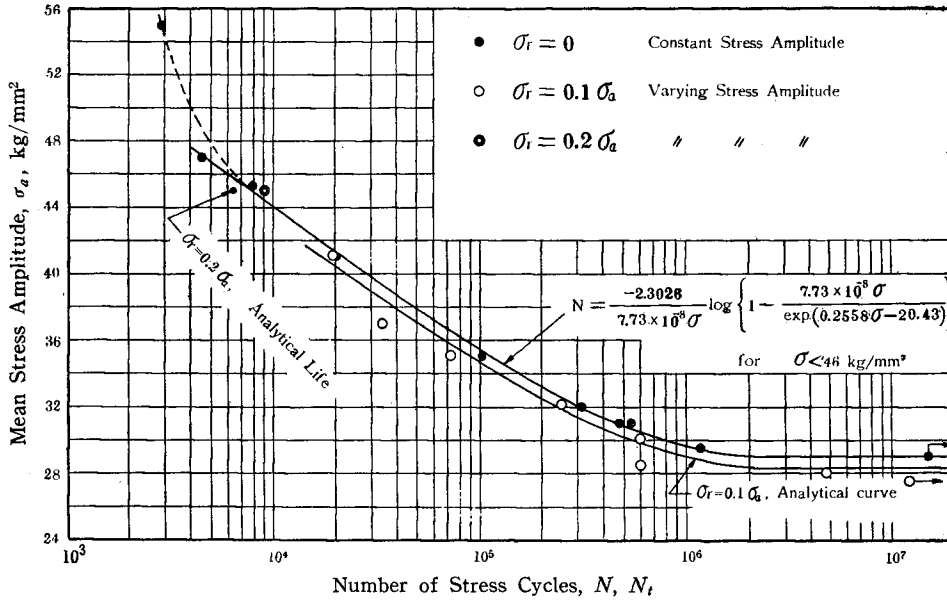were calculated by Eq. (31) and Eq. (36), and indicated in Fig. 22 by solid lines.

Fig. 22. Test results for unnotched specimens of 0.61% carbon steel under
Load Cycle I (Group B).

σ'_{wv} was determined as 31.85 kg/mm² by the analysis. The analytical fatigue lives for
$\sigma_r = 0.2\,\sigma_a$ were calculated by Eq. (35) because the major stress amplitudes were over
46 kg/mm² which was estimated to be the yield point of the material under repeated
bending.

(3)   Duralumin (Unnotched Specimen)

Tests were made of duralumin specimens, the shape being shown in Fig. 5 by
Type (b). The fatigue test results are shown in Fig. 23. From this figure it is seen
that the experimental S–N curve has the part of straight line in the stress range of
33 kg/mm² > σ > 20 kg/mm², and when σ exceeds 33 kg/mm² it bends itself upwards,
while it shows the tendency to be horizontal when σ takes the values lower than
16 kg/mm². Taking the stress level 16 kg/mm², at which the fatigue life was 6.6183
$\times 10^7$, as the fatigue limit of this material, the analytical S–N relation was obtained
from Eq. (14b) and is shown in Fig. 23.

The test results and the analytical "modified S–N curves" for $\sigma_r = 0.2$ and $0.4\,\sigma_a$,
which are worked out in the same manner as related in the preceeding sections, are
shown in Fig. 23. Both results are in good agreement to each other. The analytical
fatigue lives N_t for these cases of varying amplitude were calculated, employing the
simplified formula Eq. (33) for the stress range $\sigma_{\max} < 33$ kg/mm², and Eq. (35) for
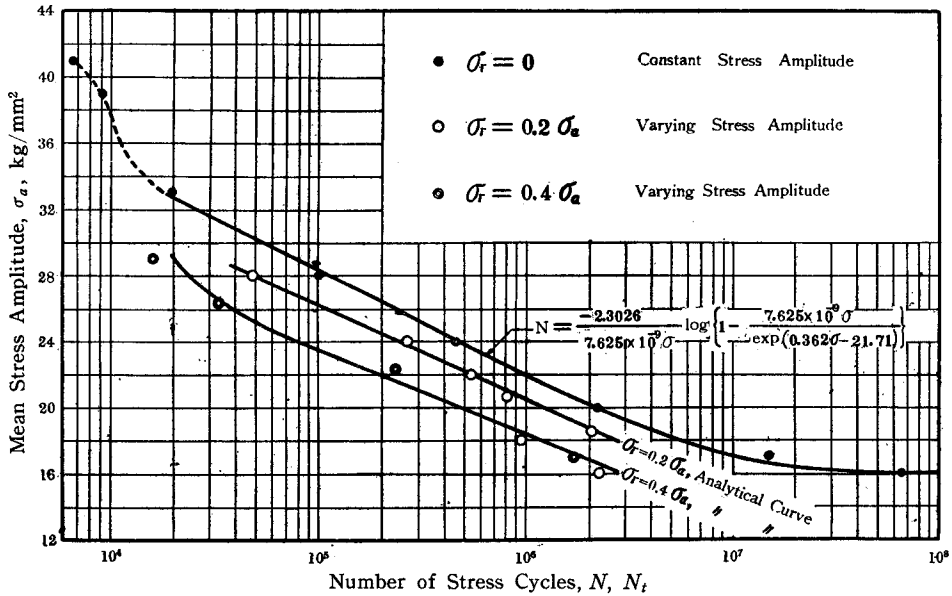the stress range $\sigma_{\max} \geqq 33$ kg/mm².

Fig. 23. Test results for unnotched specimens of duralumin under
Load Cycle I.

(4)   0.22 Per Cent Carbon Steel (Notched Specimen)

The dimensions of specimens used are shown in Fig. 5 by Type (c). The fatigue
test results for constant stress amplitude and the analytical S–N curve determined by
Eq. (47b) in Section 2.6, are exhibited in Fig. 24. The analytical S–N curve was
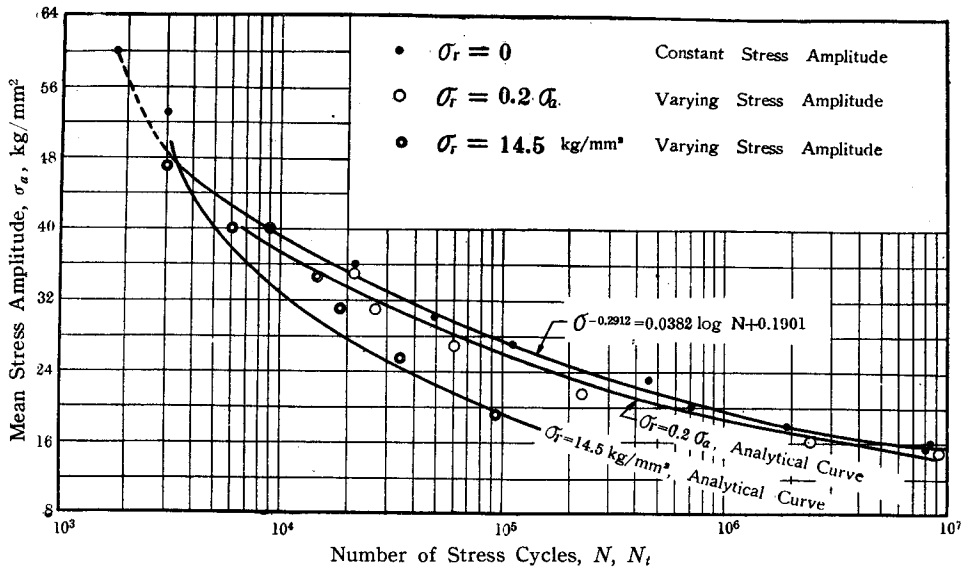

Fig. 24. Test results for notched specimens of 0.22% carbon steel under
Load Cycle I.

made by using

$$\sigma^{-0.2912} = 0.0382 \log N + 0.1901 ,$$

for the stress range $\sigma < 48 \ \text{kg/mm}^2$.

The fatigue tests were carried out for the case of varying repeated stress of $\sigma_r = 0.2 \, \sigma_a$ and $\sigma_r = 14.5 \ \text{kg/mm}^2$. The analytical fatigue lives computed according to Eq. (49) in Section 2.6, are shown by the analytical curves in Fig. 24.

3.4 Test Results by the Fatigue Testing Machine II

The unnotched specimens of Type (a) in Fig. 5 made of 0.22% carbon steel were used. In Fig. 25, the fatigue test results for constant stress amplitude are plotted by solid circles, and the analytical S–N curve according to Eq. (14b) for $\sigma < 38 \ \text{kg/mm}^2$
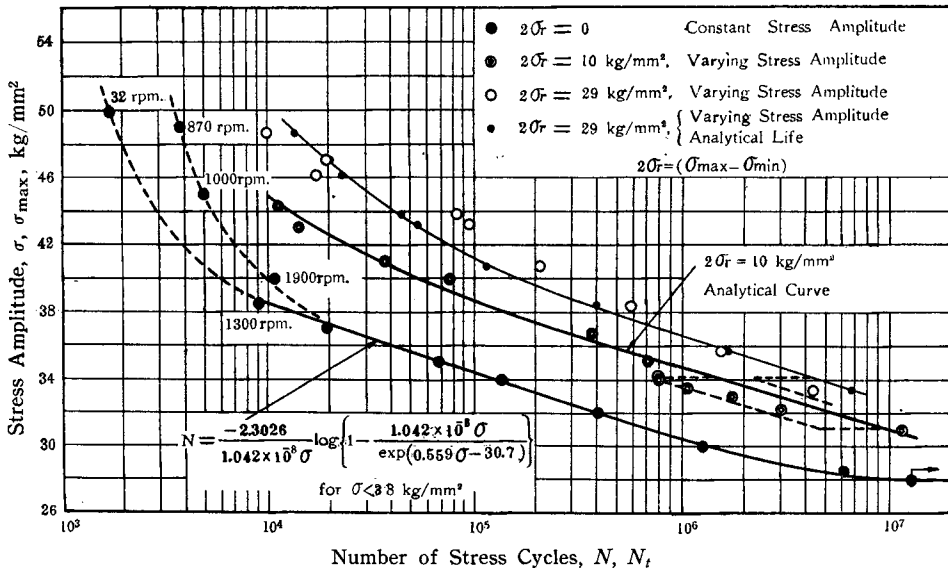

Fig. 25. Test results for unnotched specimens of 0.22% carbon steel under Load Cycle II.

and the experimental S–N curve for $\sigma \geq 38 \ \text{kg/mm}^2$ are shown by the solid curve and the dotted curves respectively. The tests in the stress range $\sigma > 38 \ \text{kg/mm}^2$ were conducted at various test speeds which were shown by the numbers close to the respective curves in the figure. $\sigma_w{}'$ determined from the test results was $28 \ \text{kg/mm}^2$, and the values of constants obtained are, $A = 0.559$, $D = -30.7$, and $m = 1.042 \times 10^{-8}$. Hence, the analyticl S–N relations were determined and shown in Fig. 25.

The another sort of fatigue tests under varying repeated stress were carried out, by keeping the variation of stress amplitude constant as $2\sigma_r = 10$ or $29 \ \text{kg/mm}^2$, and by changing the mean stress amplitude. The fatigue test results are plotted in Fig. 25,

in which the ordinate represents the maximum stress amplitude, $\sigma_{\max}$. The analytical fatigue lives for these cases were calculated by the simplest formula, Eq. (35), and the analytical "modified S-N curves" are shown by the solid curves in Fig. 25, where small solid circles exhibit the respective analytical fatigue lives for $2\sigma_r = 29\,\mathrm{kg/mm^2}$.

Since for such a stress range that the maximum stress amplitudes are between the lower and the upper yield points of the material, i.e. $\sigma_{s0} > \sigma_{\max} \geqq \sigma_{su}$, the analytical fatigue lives are computed by Eq. (66d) in Section 2.7 and applying the value $\alpha = 2$, and are shown in Fig. 25 by the dotted curves. The exact values of σ_{su} and σ_{s0} of this material had been determined by tension tests as $\sigma_{s0} = 34.2\,\mathrm{kg/mm^2}$, $\sigma_{su} = 31.1\,\mathrm{kg/mm^2}$.

3.5 Test Results by the Fatigue Testing Machine III

The study described in this section includes tests of both unnotched specimens (Type (d) in Fig. 5) and notched specimens (Type (c) in Fig. 5) of 0.22% carbon steel. The fatigue tests under alternating stresses of varying amplitude were carried out, by taking various magnitudes of maximum stress amplitude and keeping the minimum stress amplitude zero.

(1) 0.22 Per Cent Carbon Steel (Unnotched Specimen)

The fatigue test results are shown in Fig. 26. The experimental S-N curve and the "modified S-N curve" for the varying repeated stresses, which were computed
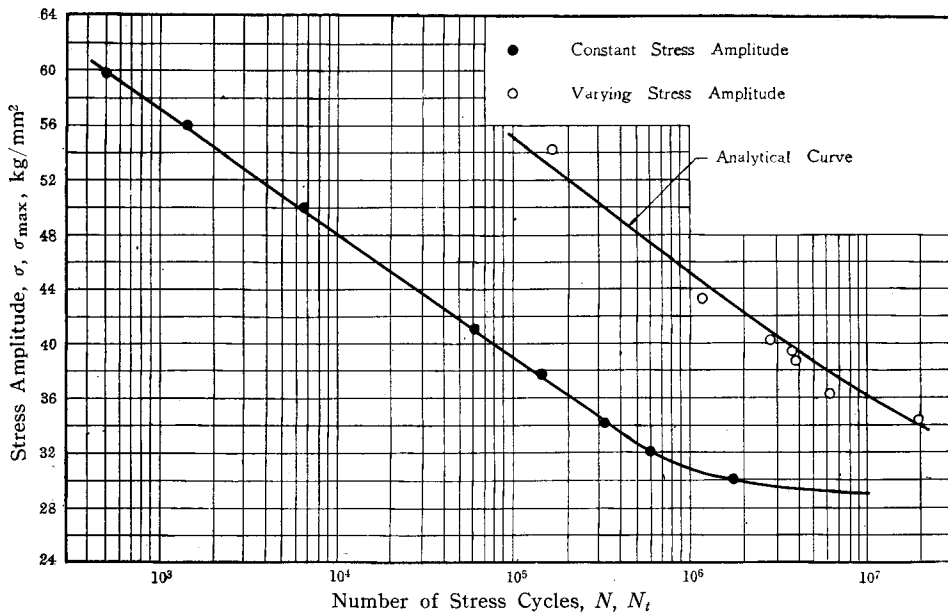

Fig. 26. Test results for unnotched specimens of 0.22% carbon steel under Load Cycle III.

by Eq. (35) referring to the experimental *S-N* curve, are also shown in this diagram. The stress-frequency diagram of this type of test indicates shuch a character that the smaller the frequency the greater the amplitude, as illustrated in Fig. 16.

(2)   0.22 Per Cent Carbon Steel (Notched Specimen)

The fatigue test results, the analytical *S-N* curve computed from Eq. (47b) in Section 2. 6, and the analytical "modified *S-N* curve" for varying repeated stresses obtained by using Eq. (49) in Section 2. 6 are altogether shown in Fig. 27.   The analytical *S-N* relation in the form,

$$\sigma^{-0.2912} = 0.0382 \log N + 0.1901$$
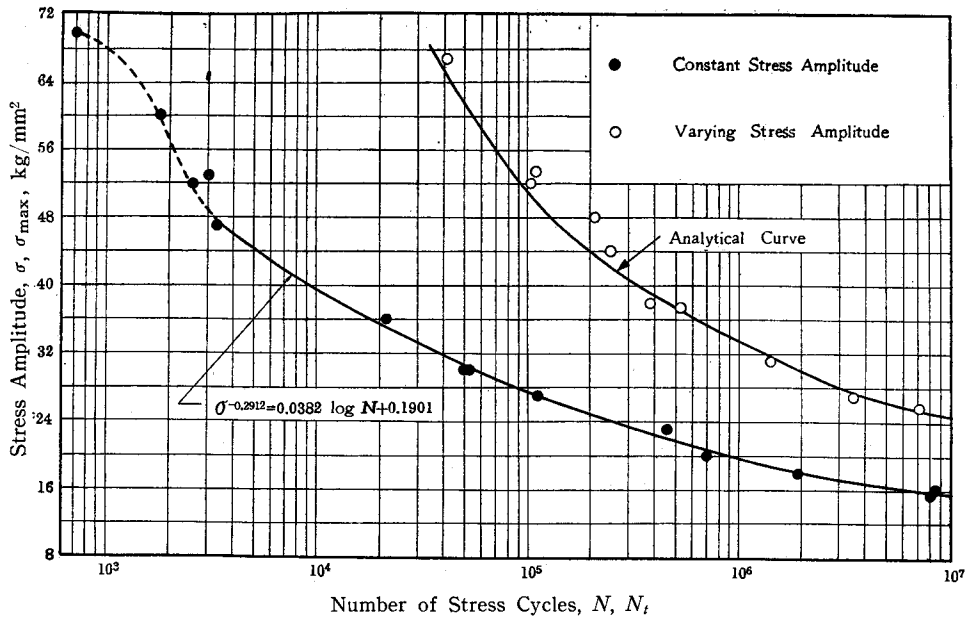
was used therin.

Fig. 27.   Test results for notched specimens of 0.22% carbon steel under
Load Cycle III.

It is understood that the analytical method given in Section 2. 6 can be applied to the estimation of fatigue strength and fatigue life of machine members which are to be used under varying repeated stresses.

IV   Summary

The fatigue tests for constant stress amplitude and also for varying stress amplitude were made of various metals, using both unnotched and notched specimens. The analytical *S-N* curves were estimated by the formula given in this paper, and the analytical fatigue lives and fatigue limits for the alternating stresses of varying

amplitude were calculated by the analytical methods established in this paper. The results obtained in this study are as follows:

(1)   Steel (Unnotched Specimen)

a.   The S–N curves were estimated by using Eq. (14b) from the conventional fatigue test results for constant stress amplitude. It was made clear that the S–N curves estimated had a fairly good agreement with the test data.

b.   The fatigue limits, $\sigma_{Wv}(\sigma'_{wv})$, for the alternating stresses of varying amplitude were computed by Eq. (36) in Chapter II. Then it was recognized that computed $\sigma_{Wv}(\sigma'_{wv})$ had a good agreement with the experimental fatigue limits.

c.   In the case of varying repeated stresses, of which the stress-cumulative frequency curve is cosinusoidal, the fatigue lives computed by Eq. (31) or Eq. (35) were a little greater than the test data, for the values of $\sigma_{\max}$ immediately above the new fatigue limit σ'_{wv}. The fatigue lives for 0.22% and 0.61% carbon steels (unnotched specimen) were computed by Eqs. (33) and (66b), and the results are illustrated in Figs. 18 and 21. From these figures, it is clear that the computed lives are a little smaller than the test data. Hence, the experimental fatigue lives are between the values computed by Eqs. (31) and (66a) and those by Eqs. (33) and (66b). So, the fatigue lives determined by employing Eqs. (33) and (66b), present the values of safety side in designing a machine member.

d.   In the stress range where the maximum stress amplitude of the varying repeated bending stresses exceeded the yield point in repeated bending of the material, the experimental fatigue lives became greater than the values computed by Eq. (35). In the practical cases, the high stresses like this would scarcely occur. But, in these cases, the fatigue lives computed by Eq. (33) will give the values of safety side in the design of machine components.

e.   The fatigue lives of the unnotched specimen of low-carbon steel subjected to the repeated bending stresses of varying amplitude, the maximum stress value being between the lower and the upper yield point, had a good agreement with the values computed by Eq. (66a) or Eq. (66d), employing $\alpha = 2$.

f.   In the stress range outside of the cases c, d, and e the fatigue lives for the varying repeated stresses had a good agreement with the values computed by Eqs. (31), (33) and (35).

Hence, it is concluded that the practical methods for the computation of fatigue strength of the materials under the alternating stresses of varying amplitude which give the values of safety side are as follows:

(i)   The fatigue limit, σ_{Wv}, for the alternating stresses of varying amplitude is calculated by Eq. (36).

(ii)   When the maximum value of varying stress amplitude exceeds the fatigue

limit, σ_{Wv}, the fatigue lives are calculated by Eq. (33).

(2)   Steel (Notched Specimen)

The *S–N* curves of the notched specimen for constant stress amplitudes were computed by Eq. (47b) in Section 2. 6, and a fairly good agreement with the test results was achieved over the stress range tested, with a few exception.   The fatigue lives of the notched specimen under the alternating stresses of varying amplitude were computed by Eq. (49), resulting in a good agreement with the experimental fatigue lives determined in the test by the fatigue testing machine I and also by the machine III.   Hence, it is concluded that the computing method by use of Eq. (49) can be adequately applied for any machine member subjected to the alternating stresses of varying amplitude of any stress–frequency curve.

(3)   Duralumin

The fatigue tests were carried out with unnotched specimens of duralumin by the fatigue testing machine I.   The experimental *S–N* curve had the tendency to become horizontal at some stress level.   Then assuming the stress at which failure does not occur at about 7×10^7 cycles as the fatigue limit, the *S–N* curve was computed by Eq. (14b) in Section 2. 1, and it showed a favourable agreement with the test results. The fatigue lives for the alternating stresses of varying amplitude were computed by Eq. (33).   It was thus clear that the computed values had a good agreement with the test results.

V   Conclusions

(1)   The functions of fatigue damage and stress history of metallic materials were established in this paper from the experimental investigations, considering the phenomena of work hardening caused by the repetition of the microscopic plastic strains of metals.   The formulas which give the analytical *S–N* curve, were obtained.

The fatigue test results were analyzed by these formulas, and it was made clear that the analytical *S–N* curves evaluated by the formulas had a fairly good agreement with the test results, not only for carbon steels but also duralumin.

(2)   The calculating methods to predict the fatigue lives and fatigue limits *versus* the alternating stresses of varying amplitude relations, were obtained by employing the functions of fatigue damage.

(3)   The fatigue tests under alternating stresses of varying amplitude were carried out by means of the specially designed fatigue testing machines of three types, using unnotched and notched specimens of 0.22% and 0.61% carbon steels and duralumin.

(4)   The results of these fatigue tests were analyzed by applying the calculating methods described, and it has been made clear that the analytical fatigue lives and

fatigue limits under varying repeated stresses had a good agreement with the test results. The simplified formulas by which the analytical fatigue lives of safety side can be computed easily, were offered.

References

1) W. Kloth und Stroppel: Kräfte, Beanspruchungen und Sicherheiten in den Landenmaschinen, Z.V.D.I., Bd. 80, Nr. 4, S. 85 (1936).

2) A. Thum und W. Bautz: Zeitfestigkeit, Z.V.D.I., Bd. 81, S. 1407 (1937).

3) B. F. Langer: Fatigue Failure from Stress Cycles of Varying Amplitude, A.S.M.E., Trans., Vol. 59, P. A-160 (1937).

4) Milton A. Miner: Cumulative Damage in Fatigue, A.S.M.E., Trans., Vol. 67, p. A-159 (1945).

5) F. E. Richart, Jr., and N. M. Newmark: An hypothesis for Determination of Cumulative Damage in Fatigue, A.S.T.M., Proc., Vol. 48, p. 767 (1948).

6) T. J. Dolan, F. E. Richart, Jr., and C. E. Work: The Influence of Fluctuation in Stress Amplitude on the Fatigue of Metals, A.S.T.M., Proc., Vol. 49, p. 646 (1949).

7) A. M. Freudental: A Random Fatigue Testing Procedure and Machine, A.S.T.M., Proc., Vol. 53, p. 896 (1953).

8) T. Nishihara, M. Kawamoto and T. Yamada: The Strength of Metals under Alternating Stresses of Varying Amplitude, Transactions of the Society of Mechanical Engineers, Japan, Vol. 10, No. 38, p. I-23 (1944).

9) T. Nishihara and T. Yamada: The Fatigue Strength of Metallic Materials under Alternating Stresses of Varying Amplitude, Transactions of the Society of Mechanical Engineers, Japan, Vol. 14, No. 47, p. I-6 (1948).

10) T. Nishihara and A. Kobayashi: New Theory of Fatigue of Metals and its Application, Transactions of the Society of Mechanical Engineers, Japan, Vol. 13, No. 44, p. 56 (1947).

11) T. Nishihara and Kawamoto: The Detection of the Fatigued Zone by a Corrosion Method, Transactions of the Society of Mechanical Engineers, Japan, Vol. 5, No. 20, p. I-43 (1939).

12) T. Nishihara and A. Kobayashi: An X-ray Study on the Fatigue of Carbon Steel, Transactions of the Society of Mechanical Engineers, Japan, Vol. 8, No. 33, p. I-194 (1942).

13) Y. Asakawa: On the Study of Fatigue of Metals, Journal of the Society of Mechanical Engineers, Japan, Vol. 36, No. 193, p. 321 (1933).

14) F. Oshiba: Degree of Fatigue in Carbon Steels under Repeated Bending, Transactions of the Society of Mechanical Engineers, Japan, Vol. 3, No. 11, p. 145 (1937).

15) F. Wever, M. Hempel und A. Schrader: Metallographische Untersuchungen über Verformungserscheinungen an der Oberfläche Biegewechselbeanspruchter Proben aus St 37, Archiv. für das Eisenhüttenwessen 26, Heft 12, S. 735 (1955).

16) H. F. Moore and T. M. Jasper: An Investigation of the Fatigue of Metals, University of Illinois Bulletin, No. 142 (1924).

17) H. F. Moore: Tests of the Fatigue Strength of Cast Iron, University of Illinois Bulletin, No. 164, p. 7 (1927).

18) J. B. Kommers: The Effect of Under-stressing on Cast Iron and Open-hearth Iron, A.S.T.M., Proc., Vol. 30, Part II, p. 368 (1930).

19) T. Nishihara and M. Kawamoto: Some Experiments on the Fatigue of Steel, Transactions of the Society of Mechanical Engineers, Japan, Vol. 6, No. 25, p. 1-47 (1940).

20) T. Nishihara and S. Taira: On the Yielding of Steel under Bending Moment, Transactions of the Japan Society of Mechanical Engineers, Vol. 18, No. 65, p. 84, p. 90 (1952).

21) K. Terazawa: The Investigation of Plasticity of Mild Steel (1944).